In-depth Identification of Pathways Related to Cisplatin-induced Hepatotoxicity through an Integrative Method Based on an Informatics-assisted Label-free Protein Quantitation and Microarray Gene Expression Approach*[S]

Young-Eun Cho‡, Thoudam S. K. Singh§, Hyun-Chul Lee¶, Pyong-Gon Moon‡, Jeong-Eun Lee‡, Myung-Hoon Lee¶, Eung-Chil Choi‖, Yu-Ju Chen, Sang-Hyun Kim§‡‡, and Moon-Chang Baek‡‡‡§§**

Cisplatin is used widely for treatment of a variety of cancer diseases. Recently, however, the use of cisplatin is restricted because of its adverse effects such as hepatotoxicity. There is no study with current proteomics technology to evaluate cisplatin-induced hepatotoxicity, even if some studies have reported on the hepatotoxicity. In this study, proteomic as well as genomic analyses have been used for identification of proteins and genes that respond to cisplatin treatment in rat primary hepatocytes. To investigate the hepatotoxic effects of cisplatin, rat primary hepatocytes were treated with an IC_{20} concentration for 24 h. From proteomic analysis based on label-free quantitation strategy, cisplatin induced 76 up-regulated and 19 down-regulated proteins among 325 distinct proteins. In the mRNA level, genomic analysis revealed 72 up-regulated and 385 down-regulated genes in the cisplatin-treated group. Based on these two analyses, 19 pathways were commonly altered, whereas seven pathways were identified only by proteomic analysis, and 19 pathways were identified only by genomic analysis. Overall, this study explained the mechanism of cisplatin-induced hepatotoxicity with two points of view: well known pathways including drug metabolism, fatty acid metabolism, and glycolysis/TCA cycle and little known pathways including urea cycle and inflammation metabolism, for hepatotoxicity of other toxic agents. Up-regulated proteins detected by proteomic analysis in the cisplatin-treated group: FBP1 (fructose 1,6-bisphosphatase 1), FASN (fatty acid synthase), CAT (catalase), PRDX1 (peroxiredoxin-1), HSPD1 (60-kDa heat shock protein), MDH2 (malate dehydrogenase 2), and ARG1 (arginase 1), and also down-regulated proteins in the cisplatin-treated group: TPM1 (tropomyosin 1), TPM3 (tropomyosin 3), and CTSB (cathepsin B), were confirmed by Western blot analysis. In addition, up-regulated mRNAs detected by microarray analysis in the cisplatin-treated group: GSTA2, GSTT2, YC2, TXNRD1, CYP2E1, CYP2C13, CYP2D1, ALDH17, ARG1, ARG2, and IL-6, and also down-regulated mRNAs: CYP2C12, CYP26B1, TPM1, and TPM3, were confirmed by RT-PCR analysis. In case of PRDX1, FASN, and ARG1, they were further confirmed by immunofluorescence analysis. Through the integrated proteomic and genomic approaches, the present study provides the first pathway map related to cisplatin-induced hepatotoxicity, which may provide new insight into the mechanism of hepatotoxicity. ***Molecular & Cellular Proteomics 11: 10.1074/mcp.M111.010884, 1–17, 2012.***

Cisplatin[1] is a potent anticancer drug used in the treatment of a wide range of cancers (1, 2). However, its significant anticancer activity and clinical use of cisplatin are often limited by its undesirable side effects, such as nephrotoxicity (3). Recent studies have suggested that hepatotoxicity is also a major dose limiting-factor when high dose cisplatin chemotherapy has been continued (4, 5). Although the nephrotoxicity of cisplatin has been well studied in clinical and basic fields, hepatotoxicity has been less studied and characterized. Liver toxicity of cisplatin is characterized by

From the ‡Department of Molecular Medicine, Cell and Matrix Biology Research Institute, School of Medicine, Kyungpook National University, Daegu 700-422, Republic of Korea, the §Department of Pharmacology, School of Medicine, Kyungpook National University, Daegu 700-422, Republic of Korea, ¶D & P Biotech, School of Medicine, Kyungpook National University, Daegu 700-422, Republic of Korea, the ‖College of Pharmacy and Research Institute of Pharmaceutical Sciences, Seoul National University, Seoul 151-742, Republic of Korea, and the **Institute of Chemistry, Academia Sinica, Taipei 11529, Taiwan

Received May 18, 2011, and in revised form, October 11, 2011
Published, MCP Papers in Press, October 24, 2011, DOI 10.1074/mcp.M111.010884

[1] The abbreviations used are: cisplatin, *cis*-diamminechloroplatinum (II); DILI, drug-induced liver injury; TEABC, triethylammonium bicarbonate; MTT, 3-[4, 5-dimethylthiazol-2-yl]-2,5-diphenyltetrazolium bromide; KEGG, Kyoto Encyclopedia of Genes and Genomes; CYP, cytochrome P-450; CoA, coenzyme A; TPM, tropomyosin.

elevation of serum transaminases, serum alkaline phosphatase, lactate dehydrogenase, bilirubin, and *c*-glutamyl transpeptidase level (6). Recent studies have focused on methods for protection of cisplatin-induced hepatotoxicity using various agents, such as selenium (7) and vitamin E (8–10). Oxidative stress has been reported to play a pivotal role as one of the most important mechanisms (11); however, the molecular mechanisms underlying cisplatin-induced hepatotoxicity have not been fully characterized.

As a result of the limitations in the current knowledge regarding the mechanisms of hepatotoxicity, drug-induced liver injury (DILI) is still a major clinical problem (12, 13). DILI is a major cause of acute liver injury, and its incidence appears to be increasing with an increase in the number of new drugs available or commonly used. DILI encompasses a variety of clinical diseases, ranging from mild biochemical abnormalities to acute liver failure. Therefore, DILI has emerged as the most frequent cause for after-marketing withdrawals of medications. Despite the rigorous preclinical and clinical review processes, DILI accounts for more than 50% of cases of acute liver failure caused by drug toxicity in the United States (14). DILI can be commonly classified into intrinsic and idiosyncratic hepatotoxicity (15–17). Intrinsic hepatotoxicity is often caused by the direct action of a drug, or more often a reactive metabolite of a drug, against hepatocytes, whereas idiosyncratic hepatotoxicity develops in only a small portion of subjects (less than one in 10,000) exposed to a drug in therapeutic doses (16). More than 1000 drugs have been associated with hepatotoxicity; however, most DILI are unpredictable and poorly understood (18). Hence, expansion of basic research into the mechanisms of DILI is warranted.

Proteomics is one of the current methods for increasing the possibility of discovery of new biomarkers and toxicity signatures. The new field of toxicoproteomics (13) offers a unique opportunity for identification of proteins/pathways in biological systems using global protein expression technologies, such as two-dimensional gel electrophoresis and mass spectrometry. In addition, it will lead to better predictive models of toxicity for use in drug development (19). Among proteomic technologies, two-dimensional gel electrophoresis has recognized changes in expression to identify several proteins with antioxidant and pro-surviving activities in the toxicology field (20). With the recent availability of techniques such as LC-MS/MS-based shotgun proteomics, which significantly increase the number of proteins identified, the more proteins related to drug toxicity mechanisms have been discovered (13). Proteomic analysis of doxorubicin-induced changes by combining two-dimensional DIGE and LC-MS/MS approaches has shown several alterations of toxicity-related proteins (21). Several integrated studies of toxicogenomics and toxicoproteomics have been conducted, such as those demonstrating acetaminophen (22) and propiconazole (23) toxicity in mouse liver. Furthermore, until now, integrated studies on proteome and genome profiling for cisplatin-induced hepatotoxicity have not been reported.

The aim of this study was to investigate the molecular events causing the hepatotoxicity of cisplatin and the underlying toxic mechanisms of cisplatin using rat primary hepatocytes. We applied an informatics-assisted label-free strategy (24–26) that adapts an efficient peptide alignment approach and spectral data validation to increase the quantitative proteomics coverage to study the cisplatin-induced proteomics alteration in hepatocytes. Treatment of cisplatin induced dramatic change in protein expression, including 76 up-regulated and 19 down-regulated proteins among a total of 325 quantified distinct proteins in primary hepatocytes. At the mRNA level, 72 up-regulated and 385 down-regulated genes in the cisplatin-treated group were identified using genomic analysis. Seven proteins and 11 genes were confirmed by Western blot and RT-PCR analysis, respectively, and three proteins were further confirmed by immunofluorescence analysis. This result would provide novel insight into the possible pathway of cisplatin-induced hepatotoxicity.

EXPERIMENTAL PROCEDURES

Materials and Reagents—Radioimmune precipitation assay buffer and protease inhibitor mixture were purchased from Cell Signaling. BCA protein assay reagent kits were obtained from Pierce. Monomeric acrylamide/bisacrylamide solution (30%, 29:1) was purchased from GenDEPOT (Barker, TX). Ammonium persulfate was purchased from Bio-Rad. SDS and DTT were purchased from USB Corp (Cleveland, OH). Trypsin (modified, sequencing grade) was obtained from Promega. Cisplatin, triethylammonium bicarbonate (TEABC), iodoacetamide, EDTA, and Tetramethylethylethylenediamine were purchased from Sigma-Aldrich. ACN, formic acid, and water of HPLC grade were purchased from Thermo Fisher Scientific. Standard protein mixture 1 (50 fmol/μl alcohol dehydrogenase, 50 fmol/μl glycogen phosphorylase b, 50 fmol/μl enolase, 50 fmol/μl serum albumin) and mixture 2 (50 fmol/μl alcohol dehydrogenase, 25 fmol/μl glycogen phosphorylase b, 100 fmol/μl enolase, 400 fmol/μl serum albumin) were purchased from Waters Corp; 0.4 fmol/μl cytosolic *Escherichia coli* digest standard proteins was also purchased from Waters Corp.

Isolation and Culture of Rat Primary Hepatocytes—All of the animal procedures have approved by the Animal Care and Use Committee at Kyungpook National University in accordance with Kyungpook National University guidelines. Hepatocytes were isolated from male Sprague-Dawley rats, weighing 200–250 g, using a two-step collagenase perfusion procedure described by the Figliomeni group (27). Hepatocyte viability, as assessed by trypan blue exclusion, exceeded 90%. Freshly harvested rat hepatocytes were suspended in William's E medium containing 5% fetal bovine serum, 100 units/ml penicillin, and 100 mg/ml streptomycin and were then inoculated in rat tail collagen-coated Petri dishes or 6-well culture plates. Hepatocytes were incubated in a humidified incubator at 95% air and 5% CO_2 at 37 °C for 24 h. After 24 h of treatment, the medium was changed, and cells were incubated with cisplatin or 0.1% Me_2SO as control in William's E medium containing 10% fetal bovine serum, 100 units/ml penicillin, and 100 mg/ml streptomycin. At 24 h, the cells were collected for various experiments according to the corresponding experimental protocol.

Cell Viability—Cell proliferation was assessed by 3-[4, 5-dimethylthiazol-2-yl]-2,5-diphenyltetrazolium bromide (MTT) assay based on metabolic reduction of MTT. Briefly, proliferation assay was per-

formed by seeding of hepatocytes (1×10^4 cells in 96-well plate) and maintenance in growth media for 24 h at 5% CO_2, 37 °C. At 80% confluence, the cells were treated with the appropriate cisplatin concentrations for 24 h followed by the addition of 20 μl of MTT solution to each well and then incubated at 37 °C for 3 h to allow for formation of formazan crystals. Excess MTT solution was removed, and filtered Me_2SO was added to each well, dissolving the formazan crystals. The plates were read on an ELISA reader (Bio-Rad) at 570 nm. The results were relatively expressed to control values specified for each experiment. Cytotoxicity was determined using the MTT reduction method and was also used for calculation of the IC_{20} of cisplatin.

Protein Preparation and Western Blot Analysis—Hepatocytes were rinsed twice with ice-cold PBS. To extract cell lysate, cell pellets were resuspended by radioimmune precipitation assay buffer (20 mM Tris-HCl, pH 7.5, 1 mM Na_2EDTA, 1 mM Na_2EDTA, 1 mM EGTA, 1% Triton, 2.5 mM sodium pyrophosphate, 2.5 mM sodium pyrophosphate, 1 mM β-glycerophosphate, 1 mM Na_3VO_4 1 μg/ml leupeptin, and 1 mM Na_3VO_4) plus protease inhibitor mixture (Cell Signaling). The samples were incubated on ice for 15 min and centrifuged at 12,000 rpm for 5 min at 4 °C, and the supernatants were then collected. Protein quantification was performed using BCA assay (Pierce).

Fifty μg of protein were denatured in SDS sample buffer and separated onto 10% SDS-polyacrylamide gels. Proteins were transferred to a nitrocellulose membrane for 60 min at 150 mA. The blots were blocked for 3 h at room temperature with 5% skim milk in PBS-T (PBS/0.1% Tween 20), washed with PBST, and incubated with primary antibodies overnight at 4 °C. The blots were washed with PBS-T and incubated with secondary antibodies conjugated by horseradish peroxidase. The blots were visualized with enhanced ECL detection reagents and quantified using ECL hyperfilm. Band volumes were measured by densitometry in at least three different experiments.

Gel-assisted Digestion—Protein concentrations of cell lysates were determined by the BCA assay before tryptic digestion. The digestion method was processed according to a gel-assisted protocol (28). Briefly, the total protein pellet was dissolved in 30 μl of 6 M urea, 5 mM EDTA, and 2% (w/v) SDS in 0.1 M TEABC and incubated at 37 °C for 30 min. The proteins were chemically reduced by the addition of 3 μl of 10 mM DTT and alkylated by the addition of 3 μl of 50 mM iodoactamide at room temperature for 30 min. The protein solution was mixed with 15 μl of acrylamide/bisacrylamide solution (30%, v/v, 29:1), 2.5 μl of 10% (w/v) ammonium persulfate, and 1 μl of 100% TEMED (tetramethylethylenediamine). The gel was cut into small pieces and washed three times with 1 ml of TEABC containing 50% (v/v) ACN. The gel samples were further dehydrated with 100% ACN and then completely dried. Proteolytic digestion was then performed with trypsin (protein:trypsin = 50:1, g/g) in 25 mM TEABC and incubated overnight at 37 °C. The peptides were extracted from the gel using sequential extraction with 100 μl of 25 mM TEABC, 100 μl of 0.1% (v/v) TFA in water, 100 μl of 0.1% (v/v) TFA in ACN, and 100 μl of 100% ACN. The solutions were combined, concentrated in a SpeedVac, and stored at −20 °C.

LC-ESI-MS/MS Analysis—Samples were reconstituted in 1 μg of peptide of buffer A (0.1% formic acid in H_2O) and analyzed by LC-MS/MS (Waters Q-TOF™ Premier from Waters Corp, Manchester, UK). Samples were injected into a 2-cm × 180-μm capillary trap column and separated by a 25-cm × 75-μm nanoACQUITY™ 1.7-μm bridged ethyl hybrid C18 column using the NanoACQUITY Ultra Performance LC™ system (Waters Corp). The column was maintained at 40 °C. Mobile phase A was composed of water with 0.1% formic acid, and mobile phase B was composed of 0.1% formic acid in acetonitrile. The peptides were separated with a gradient of 0 to 80% mobile phase B over 120 min at a flow rate of 300 nl/min, followed by a 25-min rinse with 90% of mobile phase B. The lock mass was delivered from the auxiliary NanoACQUITY pump, with a constant flow rate of 200 nl/min, at a concentration of 50 fmol [Glu1]-Fibrinopeptide B/il, to the reference sprayer of the NanoLockSpray source of the mass spectrometer. All of the samples were analyzed in triplicate. The method included a full sequential MS scan (*m/z* 150–1600, 0.6 s) and five MS/MS scans (*m/z* 100–1990, 1.2 s/scan) on the three most intense ions present in the full scan mass spectrum.

Proteomics Data Processing and Analysis—For protein identification, raw data files from MS/MS data were converted into peak lists using Mascot Distiller (Matrix Science; version 2.3.2) using the default parameters. Analysis of all MS/MS samples was performed using Mascot (Matrix Science; version 2.2.1). Mascot was set up to search the IPI_Rat_3.70 database (version 3.70; 68,161 entries), assuming trypsin as the digestion enzyme. Database search against Mascot was performed with a fragment ion mass tolerance of 0.05 Da and a parent ion tolerance of 0.1 Da. Two missed cleavages were allowed during trypsin digestion. Oxidation (Met) and carbamidomethyl (Cys) were specified as variable modification. Proteins identified with >95% confidence (for those identified with two or more peptides) or 99% confidence (for those identified by a single peptide) were included in the final data analysis. Only proteins meeting these criteria and identified in at least two independent experiments were used (29). For evaluation of the protein identification false discovery rate, we repeated searches using identical search parameters and validation criteria against a randomized decoy database created by Mascot. False discovery rates with Mascot scores ≥34 ($p < 0.05$) ranged between 0.5 and 1% in this study. MS/MS spectra and assignment for single peptide identification are included in supplemental Fig. 1.

For protein quantitation, we used IDEAL-Q software (version 1.0.1.1) to analyze the LC-MS/MS data (24–26). Briefly, raw data files from the Waters Q-Tof premier mass spectrometer were converted into files of mzXML format using Mass Wolf (Institute for Systems Biology, Seattle, WA), and the search results in Mascot were exported into the xml data format. Abundance of peptides was determined by extracted ion chromatography. The protein ratio was determined by a weighted average of the same abundance of the corresponding peptides. The final protein quantitation results were exported into an output file in the xml data format (supplemental Table II).

Microarray Analysis—Total RNA was isolated from hepatocytes using an RNeasy® mini kit (Qiagen). The quality of total RNA was determined using a Nanodrop spectrophotometer (ND-1000; Thermo Fisher Scientific) and a RNA 6000 Nano kit (Agilent Technologies, Palo Alto, CA). RNA that had a high RNA integrity number (>9.0; RNA integrity number was developed by Agilent Technologies) and an A_{260}/A_{280} absorbance ratio ranging from 1.8 to 2.1 was used for cDNA synthesis. Gene expression profiles were analyzed on a GeneChip® rat genome 230 2.0 array (Affymetrix, Santa Clara, CA) containing 31,042 probe sets. The rat genome 230 2.0 array features 31,042 probe sets representing 30,000 transcripts and variants from over 28,000 well substantiated rat genes. The Affymetrix GeneChip® procedures for generation of biotin-labeled cRNA by *in vitro* transcription, hybridization to the array, washing, and scanning were all performed according to the manufacturer's instructions. The stained GeneChip probe array was scanned with the GeneChip® Scanner 3000 (Affymetrix) 7G at 570 nm. The signal intensity of the gene expression level was calculated by Expression Console™ software, version 1.1 (30).

GenPlex™ software, version 3.0 (ISTECH Inc., Goyang, Korea), was used for analysis of the CEL file data. The MAS5 algorithm was used for the expression summary and signal calculation of the GeneChip® rat genome 230 2.0 data. Global scaling normalization was performed, and normalized data were then log-transformed with base 2 (31, 32). Differentially expressed genes were selected based on a >2.0-fold change and Welch's *t* test ($p < 0.05$). Two-fold differentially expressed genes were clustered using hierarchical clustering with the

Pearson correlation as a similarity measure and complete linkage as a linkage method. Pathway resources were provided by KEGG database.

RT-PCR Analysis—Total RNA was extracted from cultures using TRIzol reagent (Invitrogen). Reverse transcription reactions were performed in a 20-μl reaction volume containing *Taq* DNA polymerase, dNTPs, Tris-HCl (pH 9.0), KCl, $MgCl_2$, Oligo-p (dT) 1- random primer, and total RNA (1 μg) using the reaction conditions specified for the reverse transcription kit (Bioneer, Daejeon, Korea). cDNA was stored at −20 °C until future use. Resulting cDNAs were PCR-amplified using a mixture kit (Bioneer). Primer sequences were performed using gene-specific primers (supplemental Table IV). PCR conditions were 95 °C for 2 min and then 30 cycles at 95 °C for 30 s, 54 °C for 45 s, and 72 °C for 1 min with a final extension at 72 °C for 5 min. PCR products were separated onto 1.8% agarose gel, and band intensity was measured and presented by normalization with the housekeeping gene GAPDH intensity.

Immunofluorescence and Confocal Microscopy—For PRDX1 (peroxiredoxin-1), FASN (fatty acid synthase), and ARG1 (arginase 1) immunofluorescence experiments, rat primary hepatocytes were initially plated onto chamber slides with coated collagen type I (BD Bioscience, San Jose, CA). The cells were fixed in 3.7% paraformaldehyde, directly added to the culture medium for 30 min at room temperature, and then washed twice in PBS for 15 min. After washing the cells with PBS and blocking with 0.3% Triton X-100, 1.5% BSA was added to PBS for an additional 15 min. The cells were then incubated with the indicated antibodies at 4 °C overnight. Anti-PRDX1, -FASN, and -ARG1 antibodies were used at a 1:300 dilution. For detection, the cells were incubated with Alexa Fluor 488-labeled anti-rabbit secondary antibody (Invitrogen). For nuclear staining, the cells were incubated with 1 mg/ml 4′,6′-diamino-2-phenylindole for 5 min (20). The cells were washed and mounted with VECTASHIELD mounting medium (Vector Laboratories, Burlingame, CA). Images were collected using a confocal microscope (Carl Zeiss, Oberkochen, Germany) and averaged three times.

Network Analysis—The accession numbers of proteins that were significantly differently expressed after Benjamini-Hochberg adjustment were converted to entrez gene identifiers. The entrez gene identifiers from both proteins and genes analyzed KEGG pathway by the Database for Annotation, Visualization and Integrated Discovery (known as DAVID). The pathway map containing regulated-proteins/genes was drawn manually based on KEGG pathways.

Statistical Analysis—Statistical analysis was performed using the SPSS-17.0 program. For cell viability test, significant differences (*a* and *b*) are shown in relation to cisplatin treatment at $p < 0.05$ using Tukey's *post hoc* test, one-way analysis of variance (mean ± S.D., $n = 4$). For microarray and MS analysis, the data were analyzed by *t* test, and subsequently multiple testing corrections were made using the Benjamini and Hochberg false discovery rate procedure (33). For Western blot and RT-PCR analysis, Turkey's HSD (Honestly Significant Difference) test was used as a *post hoc* test if significance was detected between the control and cisplatin during the treatments at the level of $p < 0.05$ (means ± S.D., $n = 3$).

RESULTS

Cell Viability of Cisplatin-treated Primary Hepatocytes—To perform proteomic and genomic experiments with the optimal dose of cisplatin, the initial dose dependence of cisplatin capable of killing rat primary hepatocytes was determined. Analysis of cisplatin at different concentrations (0, 156.25, 312.5, 625, 1250, and 2500 μM) revealed a reduction of cell viability within a 24- treatment period (Fig. 1*A*). To investigate the hepatotoxic effect of the drug, the concentration of cisplatin (IC_{20}, 282.37 μM) for 24 h was selected for this study. We verified the toxic effect of cisplatin in primary hepatocytes by observation of cell morphology under the microscope (Fig. 1*B*). Rat primary hepatocytes without cisplatin (0.1% Me_2SO) as a control formed healthy hepatocytes, whereas cisplatin-treated primary hepatocytes died in a dose-dependent manner (Fig. 1).

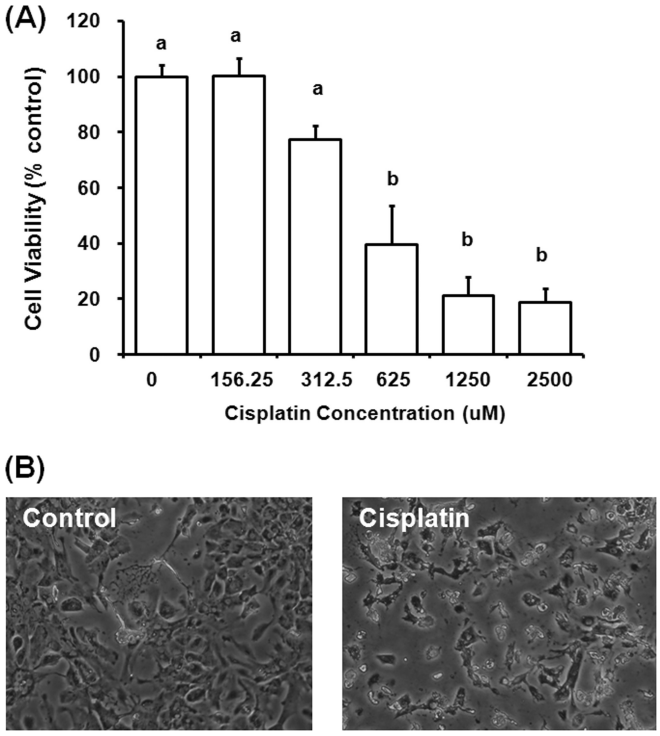

FIG. 1. **Effect of cisplatin on cell viability in rat primary hepatocytes.** *A*, rat hepatocytes were treated with different concentrations (0–2500 μM) of cisplatin for 24 h. Cell viability was detected by MTT assay, as described under "Experimental Procedures." The values are presented as percentages of control. Significant differences (*a* and *b*) are shown in relation to cisplatin treatment at $p < 0.05$ using Tukey's *post hoc* test, one-way analysis of variance (means ± S.D., $n = 4$). *B*, morphology of cisplatin-treated hepatocytes. Isolated hepatocytes were treated with 0.1% Me_2SO (control) or cisplatin (IC_{20} = 282.37 μM) for 24 h and photographed under a light microscope.

Evaluation of Quantitation Accuracy of IDEAL-Q for an Informatics-assisted Label-free Protein Quantitation—For quantitation analysis, IDEAL-Q software was used; this software has several features optimal for label-free quantitation. For improvement of quantitation accuracy, this software applies three validation criteria to the detected peptide peak clusters to filter out noisy signals, false peptide peak clusters, and coeluting peaks (24). Through the cross-assignment of commonly identified peptides and detection of unidentified peptides followed by stringent validation, IDEAL-Q can substantially increase the number of quantifiable proteins as well as the quantitation accuracy compared with other extracted ion chromatogram-based tools (24–26). Here, the quantitation accuracy and precision of IDEAL-Q for label free quantitation

were carefully examined in relation to the level of the standard mixture sample to evaluate the quantitation performance.

To determine the quantitation accuracy at the protein expression level, IDEAL-Q was applied to determine the different concentrations of the four standard proteins (glycogen phosphorylase, serum albumin precursor, enolase 1, and alcohol dehydrogenase 1) that were spiked into cytosolic *E. coli* digest standard protein (24). Ratios of the four spiked proteins were consistent with the expected ratio, with small deviations, as shown in supplemental Table I. In addition, the mean protein ratio of cytosolic 92 *E. coli* digest standard protein is in agreement with the expected ratio of 1 (1.03 ± 0.12; supplemental Fig. 2). Thus, these data confirmed that IDEAL-Q can calculate protein expression ratios with high accuracy and precision in quantitation.

Identification of Differentially Expressed Proteins in Cisplatin-treated Primary Hepatocytes—For identification of differentially expressed proteins in cisplatin-treated hepatocytes, two independent biological replicate sets from control and cisplatin-treated hepatocytes were used. Lysate samples from each group were used for gel-assisted digestion and then triplicate LC-MS/MS. By the optimized LC-MS/MS analysis mentioned above, 1887 unique peptides corresponding to distinct 485 proteins from one biological replicate set were identified ($p < 0.05$, protein score ≥ 34, false discovery rate $=$ 0.5%; supplemental Table II). Similarly, a total of 1786 peptides corresponding to 486 proteins of the other set were identified ($p < 0.05$, Protein Score ≥ 34, false discovery rate $> 1\%$; supplemental Table II). From two biological replicate sets, 325 proteins were overlapped and were subsequently adjusted for multiple testing according to the stringent method of Benjamini and Hochberg (33). In addition, the average coefficient of variation obtained for ratios of all proteins from two biological replicates (three analytical replicates) for both control and cisplatin-treated hepatocytes were determined to be 14% (corresponding to 1.2-fold change).

The cutoff criteria considered for the differentially expressed proteins were set with an adjusted *p* value (Benjamini and Hochberg (BH) *p* value) of <0.05 and a ratio of >1.8-fold difference. Finally, 95 proteins among quantified 325 proteins fulfilled the stringent cutoff criteria, and of which 76 proteins were up-regulated, whereas only 19 were down-regulated in the cisplatin-treated group. A list of these regulated proteins (95 proteins) is shown in Table I. Protein ratios were presented as cisplatin/control.

The cellular localization and molecular function of up-regulated and down-regulated proteins in cisplatin-treated primary hepatocytes were classified by gene ontology (Fig. 2). Major groups of proteins were identified in the mitochondria (26%) and organelle membrane protein (21%) (Fig. 2*A*). In addition, these proteins were found to be involved in diverse biological functions; for example, oxidation reduction, generation of precursor metabolites and energy, response to organic substance, fatty acid metabolic process, response to inorganic substance, ion transport, cofactor metabolic process, response to drug, nitrogen compound biosynthetic process, lipid catabolic process, coenzyme metabolic process, and response to hormone stimulus (Fig. 2*B*).

Gene Expression in Cisplatin-treated Primary Hepatocytes—To find significant mRNA changes in cisplatin-treated hepatocytes, three independent biological repeats were performed for microarray analysis. The rat genome 230 2.0 array providing 31,042 probe sets has been used, and each array data was analyzed by the *t* test and subsequently adjusted for multiple testing according to the stringent method of Benjamini and Hochberg (33). The cutoff criteria for significantly differentially expressed genes were set with an adjusted *p* value BH *p* value) of <0.05 and a ratio of >2-fold difference. Finally, 457 genes fulfilled the stringent cutoff criteria, and among them 72 genes were up-regulated, whereas 385 genes were down-regulated in cisplatin-treated hepatocytes (supplemental Table III).

The distribution of genes according to significance and extent of their regulation was represented in a volcano plot with BH *p* values ($-$log 10) *versus* gene ratio (presented as cisplatin/control) in cisplatin-treated primary hepatocytes (log 2) of all 457 genes (supplemental Fig. 3*A*). Next, a dendrogram was produced by hierarchical clustering of genes measured by microarray. These data showed that the gene ratios of the two groups were quite different and were separated into two distinct expression clusters (supplemental Fig. 3*B*). Gene ratios were presented as cisplatin/control.

Comparison of Proteomic and Genomic Pathways—Proteomic profiles of cisplatin-treated hepatocytes were obtained using high throughput nano LC-MS/MS, whereas genomic profiles were obtained using microarray. KEGG pathway analyses based on proteomic and genomic data showed various common pathways (Table II), including drug metabolism, metabolism of xenobiotics by cytochrome P-450, metabolism of biochemical intermediates (*e.g.* ascorbate and aldarate, β-alanine, butanoate, fatty acid, retinol, and tryptophan), cardiac muscle contraction, biosynthesis of biochemical intermediates (*e.g.* unsaturated fatty acids and primary bile acid), glycolysis, TCA cycle, oxidative stress (*e.g.* Alzheimer, Huntington, and Parkinson disease), fatty acid elongation in mitochondria, oxidative phosphorylation, peroxisome proliferator-activated receptor signaling pathway, and amino acid degradation. A KEGG pathway based on proteomics analysis gave a series of unique pathways with fatty acid elongation in mitochondria, lysine degradation, pentose and glucuronate interconversions, steroid hormone biosynthesis, and metabolism of biochemical intermediates (*e.g.* porphyrin and chlorophyll, propanoate, starch, and sucrose). Genomic analysis also gave a series of unique pathways with focal adhesion, cytokine-cytokine receptor interaction, cell cycle, ECM-receptor interaction, vascular smooth muscle contraction, leukocyte transendothelial migration, melanogenesis, viral myocarditis, melanoma, complement and coagulation cas-

TABLE I

List of differentially expressed proteins (76 up-regulated and 19 down-regulated) in cisplatin-treated rat primary hepatocytes based on biological function

Proteins from two independent biological replicate sets from control and cisplatin-treated hepatocytes were used for gel-assisted digestion and then triplicate LC-MS/MS analysis. IDEAL-Q software was applied for the label-free quantitation strategy.

(Gene symbol) protein name	Ratio (cisplatin-treated/control)	S.D.	Accession number	Protein score
Carbon dioxide metabolism				
(Car3) Carbonic anhydrase 3	1.8	0.23	IPI00230788	84
Cardiac muscle contraction (hepatic fibrost)				
(Gfap) Isoform 1 of glial fibrillary acidic protein	3.0	1.46	IPI00190943	41
(Myl6l) Myosin light polypeptide 6	2.2	0.40	IPI00365944	79
(Tubb3) Tubulin β-3 chain	2.1	0.14	IPI00362160	193
(Usmg5) Up-regulated during skeletal muscle growth protein 5	2.0	0.33	IPI00202111	85
(Tuba1a) Tubulin α-1A chain	1.8	1.24	IPI00189795	150
(Tubb6) Tubulin, β6	1.8	0.11	IPI00195673	156
(Tagln) Transgelin	0.5	0.07	IPI00231196	118
(Ctnna1) Catenin (cadherin-associated protein), α1, isoform CRA_b	0.5	0.06	IPI00358406	67
(Clu) Clusterin	0.5	0.20	IPI00198667	62
(Lmna) Lamin-A	0.5	0.08	IPI00201060	196
(Tpm3) Isoform 2 of tropomyosin α-3 chain	0.4	0.05	IPI00210941	120
(Cald1) Nonmuscle caldesmon	0.3	0.20	IPI00208118	343
(Tpm1) Tropomyosin 1 α chain isoform c	0.3	0.03	IPI00210945	320
Drug metabolism (detoxification)				
(Ugt2b36) UDP-glucuronosyltransferase 2B4	2.8	0.64	IPI00203473	308
(Gstz1) RCG20683 Isoform CRA_b	2.5	0.67	IPI00763872	115
(Ugt2b17) UDP-glucuronosyltransferase 2B1	2.5	0.89	IPI00190402	181
(Cyp2d1) Cytochrome P-450 2D1	2.2	1.03	IPI00324443	347
(Pon1) Serum paraoxonase/arylesterase 1	2.1	0.54	IPI00555299	229
(Ugt2b34) Similar to UDP glucuronosyltransferase 2 family, polypeptide B34	2.1	0.32	IPI00554004	109
(Ces3) Carboxylesterase 3	1.9	0.13	IPI00326972	142
(Ugt1a1) UDP-glucuronosyltransferase 1–1	1.9	0.22	IPI00213569	575
(Cyp2c13) Cytochrome P-450 2C13, male-specific	1.8	0.01	IPI00325874	123
(Ugt2b36) UDP glucuronosyltransferase 2 family, polypeptide B36	1.8	0.15	IPI00471524	261
(Es22) Liver carboxylesterase 4	1.8	0.01	IPI00679256	225
Fatty acid metabolism				
(Fasn) Fatty acid synthase	3.8	0.71	IPI00200661	46
(Fabp1) Fatty acid-binding protein	3.2	1.15	IPI00190790	55
(Adh1) Alcohol dehydrogenase 1	2.7	0.95	IPI00331983	73
(Hsd17b12) Estradiol 17-β-dehydrogenase 12	2.0	0.16	IPI00208645	58
(Mttp) Microsomal triglyceride transfer protein	1.8	0.02	IPI00212316	262
(Apob) Apolipoprotein B-100	1.8	0.33	IPI00555161	41
Fatty acid metabolism (β-oxidation)				
(LOC683474) Similar to aldehyde dehydrogenase 8 family	3.1	0.17	IPI00359623	124
(Acox2) Peroxisomal acyl-coenzyme A oxidase 2	3.0	0.58	IPI00205561	59
(Hadh) Hydroxyacyl-coenzyme A dehydrogenase	2.5	0.63	IPI00205157	446
(Ehhadh) Peroxisomal bifunctional enzyme	2.1	0.15	IPI00232011	102
(Ech1) δ(3,5)-δ(2,4)-dienoyl-CoA isomerase	1.9	0.03	IPI00326561	70
(Dci) 3,2-*trans*-Enoyl-CoA isomerase	1.8	0.13	IPI00215574	113
(Decr1) 2,4-Dienoyl-CoA reductase	1.8	0.18	IPI00213659	143
(Echs1) Enoyl-CoA hydratase	1.8	0.07	IPI00207217	298
(Pccb) Propionyl coenzyme A carboxylase, β polypeptide	1.8	0.46	IPI00851115	62
Glycolysis				
(Fbp1) Fructose-1,6-bisphosphatase 1	4.1	0.90	IPI00231745	84
(RGD) Similar to glyceraldehyde-3-phosphate dehydrogenase	2.1	0.31	IPI00554039	226
Oxidative stress				
(Prdx5) Peroxiredoxin-5	3.6	0.29	IPI00205745	112
(LOC684747) Similar to 60-kDa heat shock protein	3.2	1.23	IPI00763910	1391
(Prdx1) Peroxiredoxin-1	1.9	0.02	IPI00211779	108
(Cat) Catalase	1.8	0.12	IPI00231742	639
Oxidative phosphorylation				
(Uqcrc1) Cytochrome *b*-c_1 complex subunit 1	2.6	0.26	IPI00471577	235
(Atp5o) ATP synthase subunit O	2.0	0.10	IPI00195123	326
(Mt-co2) Cytochrome *c* oxidase subunit II	2.0	0.33	IPI00734686	229
(Atp5i) ATP synthase subunit e	2.0	0.33	IPI00231978	88
(Mt-nd1) NADH dehydrogenase subunit 1	2.0	0.18	IPI00734781	57

TABLE I—*continued*

(Gene symbol) protein name	Ratio (cisplatin-treated/control)	S.D.	Accession number	Protein score
(Atp5l) ATP synthase, H+ transporting	1.8	0.08	IPI00421711	68
(Atp5a1) ATP synthase subunit α	1.8	0.19	IPI00396910	1191
(Ndufv2) NADH dehydrogenase [ubiquinone] flavoprotein 2	1.8	0.20	IPI00367152	85
(Ndufa9) Ndufa9 protein	1.8	0.01	IPI00358441	120
Primary bile acid biosynthesis				
(Akr1c1) 4,3-α-hydroxysteroid dehydrogenase	2.3	0.09	IPI00211100	136
(Baat) Bile acid-CoA:amino acid *N*-acyltransferase	2.0	0.36	IPI00207010	100
(Slc27a5) Bile acyl-CoA synthetase	1.8	0.04	IPI00191416	223
Pro-oncogene				
(Abl1) ABL1 (Fragment)	1.9	0.19	IPI00370643	37
(Ctsb) Cathepsin B	0.4	0.05	IPI00212811	81
Retinol and cystein metabolism				
(Rdh7) Retinol dehydrogenase 3	1.8	0.16	IPI00195585	187
(Cth) Cystathionine γ-lyase	1.8	0.07	IPI00194550	57
(Ncl) Nucleolin	0.4	0.06	IPI00231827	56
Starch and sucrose metabolism				
(Npl2) *N*-Acetylneuraminate pyruvate lyase 2	1.9	0.28	IPI00560967	287
Signaling regulator				
(Ahnak) AHNAK 1 (fragment)	0.2	0.06	IPI00564413	181
Steroid hormone biosynthesis				
(Hsd11b1) Isoform 11-HSD1A of corticosteroid 11-β-dehydrogenase isozyme 1	3.3	0.18	IPI00211096	93
TCA cycle				
(Mdh2) Malate dehydrogenase, mitochondrial	1.9	0.10	IPI00197696	734
(Aco2) Aconitate hydratase	2.0	0.45	IPI00421539	260
Transcription				
(LOC680312) Histone H2B	4.0	0.01	IPI00190348	129
(RGD1564767) Histone H2A	3.8	1.21	IPI00188688	125
(Rap1a) Ras-related protein Rap-1A	3.1	1.14	IPI00187747	55
(Rps4x) 40 S ribosomal protein S4, X isoform	1.8	0.08	IPI00475474	43
(Luzp1) Leucine zipper protein 1	0.4	0.09	IPI00324444	55
(Hnrnpf) Heterogeneous nuclear ribonucleoprotein F	0.4	0.04	IPI00210357	168
(Hnrnpab) Nucleic acid-binding factor pRM10	0.3	0.02	IPI00208193	106
(Hnrnpa2b1) Isoform B0b of heterogeneous nuclear ribonucleoproteins A2/B1	0.3	0.03	IPI00212969	238
Transferase and binding protein				
(Bhmt) Betaine–homocysteine *S*-methyltransferase 1	3.4	0.27	IPI00332027	284
(Ssr1) Translocon-associated protein subunit α	2.9	0.06	IPI00364884	113
(RGD1308874) Isoform 2 of adipocyte plasma membrane-associated protein	2.6	0.36	IPI00382223	78
(RGD1309676) Uncharacterized protein C10orf58 homolog	2.6	0.53	IPI00364616	63
(Slc25a10) Solute carrier family 25 (mitochondrial carrier)	2.1	0.05	IPI00209363	243
(Ssr4) Translocon-associated protein subunit delta	2.1	0.16	IPI00949999	35
(Comt) Isoform 1 of catechol *O*-methyltransferase	1.9	0.03	IPI00210280	88
(Cd81) CD81 antigen	1.8	0.29	IPI00208154	36
(Slc25a1) Tricarboxylate transport protein	1.8	0.19	IPI00327694	74
(Slc25a13) Similar to calcium-binding mitochondrial carrier protein Aralar2	1.8	0.17	IPI00358163	672
(Cand1) Cullin-associated NEDD8-dissociated protein 1	1.8	0.08	IPI00205466	49
(Suox) Sulfite oxidase, mitochondrial	0.5	0.19	IPI00193919	33
(Ptbp1) Isoform PYBP1 of polypyrimidine tract-binding protein 1	0.5	0.05	IPI00231555	85
(Ddx5) Ddx5	0.3	0.05	IPI00464718	62
(Basp1) Brain acid-soluble protein 1	0.1	0.04	IPI00231651	179
(Ybx1) Ybx1 protein	0.1	0.06	IPI00551815	64
(Sfxn1) Sideroflexin-1	1.9	0.09	IPI00213735	138
Urea cycle				
(Arg1) Arginase-1	2.8	0.57	IPI00327518	214
(Ass1) Argininosuccinate synthase	1.8	0.00	IPI00211127	161

cades, glioma, bladder cancer, pathways in cancer/nitrogen metabolism/metabolic, metabolism of glutathione/nitrogen, and a number of additional signaling pathways (calcium, chemokine, p53, and TGF-β signaling). In this study, to explain the mechanism of cisplatin-induced hepatotoxicity, we focused on well known pathways including drug metabolism, fatty acid metabolism, and glycolysis/TCA cycle, as well as little known pathways including urea cycle and inflammation

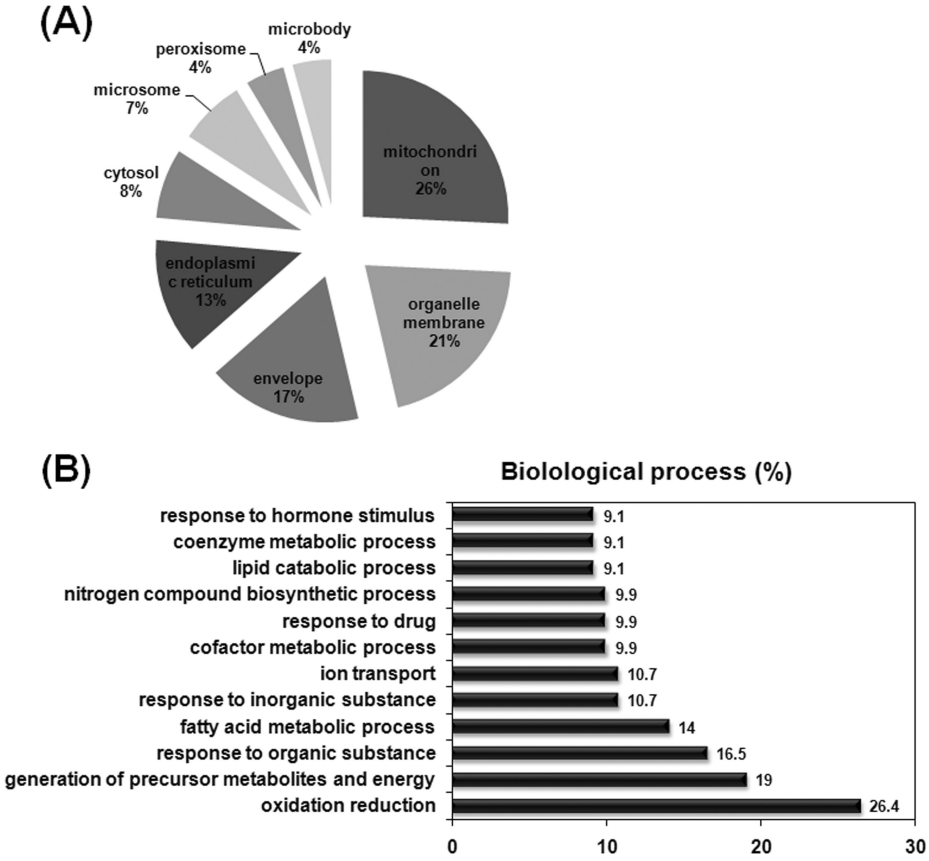

FIG. 2. **Subcellular localization (*A*) and classification based on the molecular function (*B*) of proteins differentially regulated by cisplatin.**

metabolism pathways, for hepatotoxicity of other toxic agents (Table III).

Validation of Protein Expression Changes Using Western Blot—To further enhance the possibility that our study would facilitate candidate identification for toxicity markers and to lead to a new and improved explanation of the cisplatin-induced toxic mechanisms, some proteins differentially expressed by proteomics analysis were confirmed by Western blot. FBP1 (fructose 1,6-bisphosphatase 1), FASN (fatty acid synthase), CAT (catalase), PRDX1 (peroxiredoxin-1), HSPD1 (60-kDa heat shock protein), MDH2 (malate dehydrogenase 2), and ARG1 (arginase 1) were selected based on several criteria, including: 1) proteins belong to drug metabolism, fatty acid metabolism, glycolysis/TCA cycle, urea cycle, and inflammation metabolism pathways, which may enable their use as DILI biomarkers; 2) their potential roles in contributing to DILI prediction as liver injury proteins; and 3) the availability of commercial antibodies.

By Western blot, protein levels of FBP1, FASN, CAT, PRDX1, HSPD1, MDH2, and ARG1 were significantly higher in the cisplatin-treated group than in the control, as determined by MS analysis (Fig. 3). In addition, we also checked down-regulated proteins in cisplatin-treated group and selected three proteins, namely CTSB (cathepsin B), TPM1 (tropomysin 1), and TPM3 (tropomysin 3). As expected, the down-regulated levels detected by Western blot analysis were similar to those detected by MS analysis (Fig. 3). The similarity of fold changes between Western blot and mass analysis results might demonstrate the validity of our IDEAL-Q quantitation strategy. These results suggested that other proteins identified by LC-MS/MS could also serve as potential markers in future studies of cisplatin.

Validation of Gene Expression Changes Using RT-PCR—GSTA2, GSTT2, YC2, TXNRD1, CYP2E1, CYP2C13, CYP2D1, ALDH1A7, ARG1, ARG2, and IL-6 were selected based on several criteria mentioned above to validate genomics results. mRNA levels of these genes were increased in cisplatin-treated cells and confirmed by RT-PCR (Fig. 4). RT-PCR indicated that the mRNA levels of GST isoforms were significantly increased in hepatocytes after treatment with cisplatin for 24 h ($p < 0.05$), verifying microarray data. mRNA levels of CYP2D1 and CYP2C13, up-regulated in MS data, and CYPE1, 1.6-fold up-regulated in microarray data, were significantly increased in cisplatin-treated hepatocytes by RT-PCR. In particular, mRNA levels of ARG1, up-regulated in MS data, and ARG2, up-regulated in microarray data, were increased in cisplatin-treated hepatocytes. Elevation of IL-6 transcript levels, as shown in microarray data, was confirmed by RT-PCR. mRNA levels of TXNRD1 and ALDH1A7, up-regulated in microarray data, were confirmed by RT-PCR. In addition, we also checked down-regulated mRNAs in cisplatin-treated group from microarray data. The down-regulation of four

TABLE II

Comparison of protein and gene expression profiles in rat primary hepatocytes treated with cisplatin ($p < 0.05$)

Each pathway was statistically significant by a KEGG pathway using DAVID program (*t* test with *p* value).

KEGG pathways	*p* value of proteins	Also present in transcript analysis[a]	*p* value of genes
Alzheimer disease	2.0E-02	○	2.9E-02
Ascorbate and aldarate metabolism	7.5E-04	○	5.0E-02
β-Alanine metabolism	2.4E-02	○	1.0E-02
Biosynthesis of unsaturated fatty acids	2.8E-02	○	2.9E-02
Butanoate metabolism	5.3E-03	○	8.2E-03
Cardiac muscle contraction	5.0E-02	○	4.2E-03
Drug metabolism	1.0E-04	○	4.0E-03
Fatty acid elongation in mitochondria	8.4E-03		
Fatty acid metabolism	8.2E-05	○	1.2E-02
Glycolysis	3.4E-02	○	6.6E-03
Huntington disease	5.5E-03	○	7.0E-03
Lysine degradation	7.3E-03		
Metabolism of xenobiotics by cytochrome P-450	4.0E-03	○	1.5E-03
Oxidative phosphorylation	6.6E-04	○	9.4E-03
Parkinson disease	4.3E-03	○	8.0E-03
Pentose and glucuronate interconversions	5.1E-04		
Porphyrin and chlorophyll metabolism	4.5E-03		
Peroxisome proliferator-activated receptor signaling pathway	7.2E-03	○	3.4E-02
Primary bile acid biosynthesis	1.1E-02	○	3.0E-02
Propanoate metabolism	5.3E-03		
Retinol metabolism	4.2E-04	○	5.0E-02
Starch and sucrose metabolism	7.4E-03		
Steroid hormone biosynthesis	5.9E-06		
TCA cycle	9.3E-03	○	5.0E-02
Tryptophan metabolism	1.1E-02	○	6.6E-03
Valine, leucine, and isoleucine degradation	1.5E-03	○	2.6E-02

[a] Pathways based on genomics analyses from supplemental Table III. Bold type indicates pathways whose functions are evaluated in the current study.

mRNAs, namely CYP2C12, CYP26B1, TPM1, and TPM3, was also confirmed by RT-PCR (Fig. 4). In conclusion, the consistency between RT-PCR and microarray quantitation demonstrated the validity of our microarray quantitation.

Validation of Protein Expression Changes Using Immunofluorescence Analysis—Immunofluorescence confocal microscopy was used to investigate localization and possible abundance of cytoplasmic proteins in cisplatin-treated hepatocytes. Fluorescence data for subcellular localization of three proteins, PRDX1, FASN, and ARG1, was observed in the cytoplasm, and significantly increased fluorescence intensity was also observed in cisplatin-treated hepatocytes (Fig. 5). These general trends were reproduced in at least two independent experiments using this sensitive visualization technique.

Protein Networks—To better understand the interactions between differentially expressed proteins in response to cisplatin treatment, networks of inter-relationships of these proteins and genes were constructed using the KEGG pathway program. Proteins and genes belong to drug metabolism, fatty acid metabolism, glycolysis and TCA cycle, urea cycle, and inflammation metabolism pathways derived from proteomic and genomic analysis are shown in Table III. Therefore, these biochemical pathways show a hypothetical complex pathway built based on proteins and genes, confirmed by Western blot and RT-PCR, from our experiments (Fig. 6), and the explanation of each protein belonging to specific pathways has been described in the discussion section.

DISCUSSION

DILI is still unpredictable, because the mechanisms of drug toxicity pathways were not clearly characterized until now. Many attempts have been made to uncover the pathways of DILI, and these attempts have focused on some specific pathways. Recently, the advent of global proteomics profiling, based on two-dimensional gel electrophoresis and MALDI-TOF, and nano LC-MS/MS methods allows the identification of global proteins affected by DILI. In the present study, we used a proteomic approach based on nano LC-MS/MS with IDEAL-Q software for an informatics-assisted label-free protein quantitation in cisplatin-treated rat primary hepatocytes. In addition, we extended to genomic studies using a microarray method to understand the more detailed toxic pathways. Some studies of the drug toxicity of several drugs, including acetaminophen (22), propiconazole (23), and methapyrilene (34), have reported on use of proteomic or genomic profiles of mouse and rat liver. However, no proteomic analysis for evaluation of cisplatin-induced hepatoxicity has been reported, and this paper is the first report that systematically examines

TABLE III
List of proteins and genes belong to representative pathways derived from proteomic and genomic analysis

Protein name	Gene name	Protein[a]	Gene[b]
Drug metabolism/oxidative stress			
Mitochondrial of peroxiredoxin-5	PRDX5	3.6	0.9
Peroxiredoxin-1	PRDX1	1.9	1.2
Catalase	CAT	1.8	1.8
Superoxide dismutase [Mn], mitochondrial	SOD2	1.6	0.9
60-kDa heat shock protein, mitochondrial	HSPD1	1.5	ND
Glutathione *S*-transferase $\alpha 2$	GSTA2	ND	2.9
Glutathione *S*-transferase $\theta 2$	GSTT2	ND	2.4
Glutathione *S*-transferase Yc2 subunit	YC2	ND	2.0
Thioredoxin reductase 1	TXNRD1	ND	2.0
Metallothionein 1A	MT1A	ND	2.4
Metallothionein 2A	MT2A	ND	2.3
70-kDa heat shock protein 1	Hspa1	ND	4.6
Cytochrome P-450, family 2, subfamily d, polypeptide 1	CYP2D1	2.2	1.3
Cytochrome P-450, family 2, subfamily c, polypeptide 13	CYP2C13	1.8	1.6
Cytochrome P-450, family 2, subfamily d, polypeptide 5	CYP2D5	1.5	ND
Cytochrome P-450, family 2, subfamily e, polypeptide 1	CYP2E1	ND	1.6
Cytochrome P-450, family 4, subfamily a, polypeptide 1	CYP4A1	ND	1.6
Cytochrome P-450, family 2, subfamily c, polypeptide 12	CYP2C12	ND	0.5
Cytochrome P-450, subfamily IIC (mephenytoin 4-hydroxylase)	CYP2C	ND	0.4
Cytochrome P-450, family 26, subfamily b, polypeptide 1	CYP26B1	ND	0.3
Fatty acid metabolism			
Fatty acid synthase	FASN	3.8	2.6
Fatty acid-binding protein	FABP1	3.2	1.5
Alcohol dehydrogenase 1	ADH1	2.7	1.4
Estradiol 17-β-dehydrogenase 12	HSD17B12	2.0	ND
Microsomal triglyceride transfer protein	MTTP	1.8	ND
Apolipoprotein B-100	APOB	1.8	1.6
Aldehyde dehydrogenase family 1, member A1	ALDH1A1	ND	3.9
Aldehyde dehydrogenase family 1, subfamily A7	ALDH1A7	ND	2.1
Acetyl-coenzyme A acyltransferase 2	ACAA2	ND	2.1
Glycolysis/TCA cycle			
Fructose-1,6-bisphosphatase 1	FBP1	4.1	1.6
Malate dehydrogenase, mitochondrial 2	MDH2	1.9	1.1
Isocitrate dehydrogenase 1 (NADP+), soluble	IDH1	ND	2.0
Urea cycle and inflammation metabolism			
Arginase 1	ARG1	2.8	1.3
Arginase 2	ARG2	ND	2.7
Interleukin 6	IL-6	ND	2.7
Argininosuccinate synthase	ASS1	1.8	ND

[a] The cisplatin/control ratio at protein level was measured by MS/MS analysis. ND indicates not detected protein.
[b] The cisplatin/control ratio at mRNA level was measured by microarray analysis. ND indicates not detected gene.

hepatotoxic responses induced by the cisplatin using an integrated toxicoproteomic and toxicogenomic approach. In this study, we found that 26 and 38 pathways in cisplatin-treated hepatocytes were differentially expressed by proteomic and genomic analysis, respectively. Among them, 19 pathways were similarly altered by two omics analyses, whereas 7 and 19 pathways were only identified by proteomic and genomic analysis, respectively.

It has been reported that gene expression analysis does not necessarily reflect changes in corresponding proteins and cellular function, and there is some evidence of poor correlation between mRNA and protein abundance (23, 35). This lack of strong correlation might come from mRNA degradation, alternative splicing, or post-transcriptional regulation of gene expression. Despite the known low correlation between two omics analyses, this study showed that the number of up-regulated proteins (76 proteins) was higher than down-regulated proteins (19 proteins) after cisplatin treatment, whereas the number of up-regulated genes (72 genes) was smaller than down-regulated genes (385 genes). To define the reason for this discrepancy, up- and down-regulated genes were compared with up- and down-regulated proteins, respectively, based on cellular locations and biological functions using IPA software (Ingenuity Systems). The number of up-regulated genes was similar to that of proteins, and the locations and biological functions of these genes showed patterns similar to those of proteins (supplemental Table V, *A* and *B*). However, the number of down-regulated genes and proteins

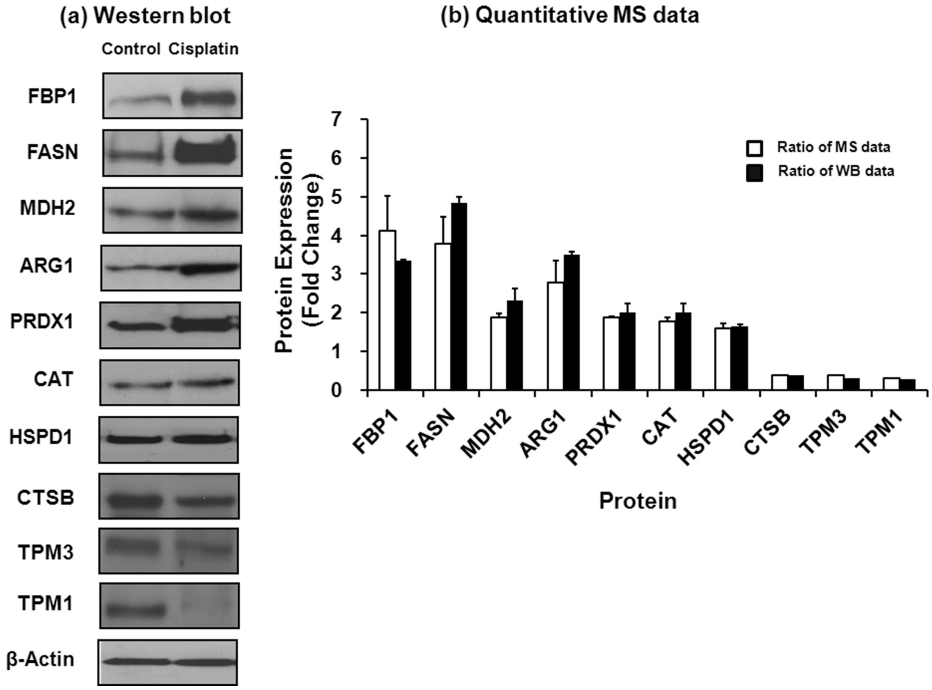

FIG. 3. **Western blot analysis of representative proteins identified by LC-MS/MS.** *a*, differential expression level of proteins, including FBP1, FASN, MDH2, ARG1, PRDX1, CAT, and HSPD1 were detected by Western blot analysis. Rat hepatocytes were treated with 0.1% Me_2SO (control) or 282.37 μM cisplatin (IC_{20}) for 24 h, respectively. After cell lysis, 50 μg of whole cell extract were separated by SDS-PAGE. For densitometric evaluation of the respective ECL signals, ImageQuant software was used with normalization to β-actin. Each blot shows a representative result among three independent experiments. *b*, results derived from Western blot analysis (*black bars*, $n = 3$) were compared with those from MS analysis (*white bars*, $n = 2$).

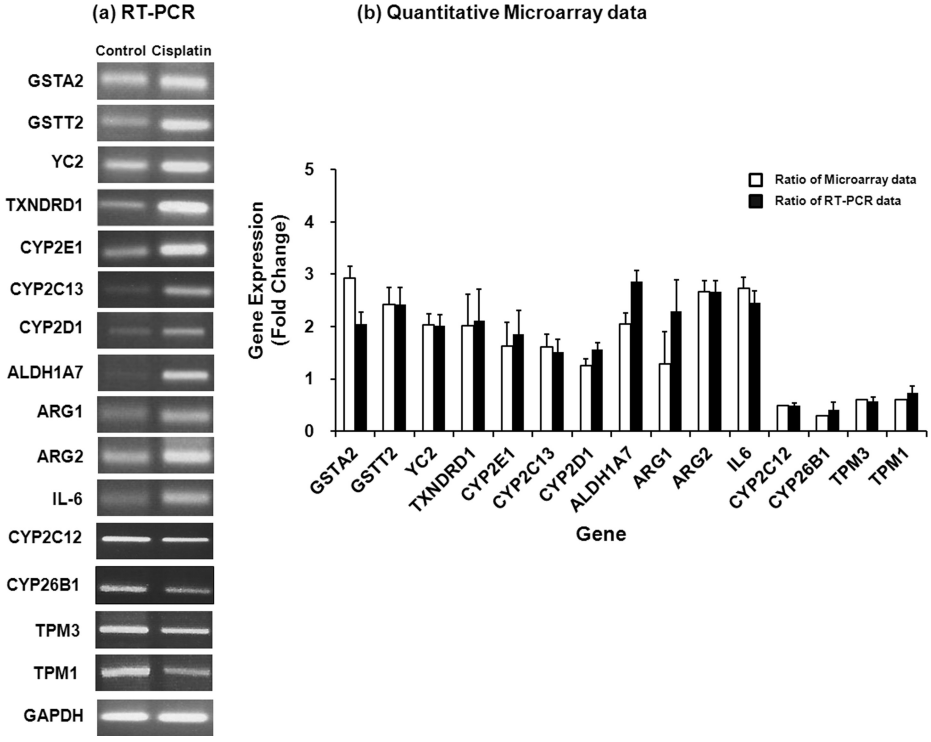

FIG. 4. **RT-PCR analysis of representative genes identified by microarray.** *a*, differential expression level of genes, including GSTA2, GSTT2, YC2, TXNRD1, CYP2E1, CYP2C13, CYP2D1, ALDH1A7, ARG1, ARG2, and IL-6 were detected by RT-PCR. Rat hepatocytes were treated with 0.1% Me_2SO (control) or 282.37 μM cisplatin (IC_{20}) for 24 h, respectively. Total RNAs were extracted from each cell and amplified by corresponding primers for each gene. RT-PCR products were separated on 1.8% agarose gel, and band intensity was measured and presented by normalizing with housekeeping gene, GAPDH. Each RT-PCR shows a representative result of three independent experiments. *b*, results derived from RT-PCR analysis (*black bars*, $n = 3$) were compared with those from microarray analysis (*white bars*, $n = 3$).

showed a big difference, although several factors mentioned above might explain this low correlation between two omics analysis. Interestingly, we found that there were some differences of cellular locations and biological functions between down-regulated genes and proteins (supplemental Table V, *C* and *D*). The locations of 385 down-regulated genes analyzed by IPA software were classified into the cytoplasm (99 genes), nucleus (69 genes), plasma membrane (152 genes), and unknown (65 genes) (supplemental Table VC). However, the locations of 19 down-regulated proteins were classified into the cytoplasm (6 proteins), nucleus (10 proteins), and plasma membrane (3 proteins) (supplemental Table VC). Among 320 down-regulated genes excluding unknown genes (65 genes), almost 30% of genes encode

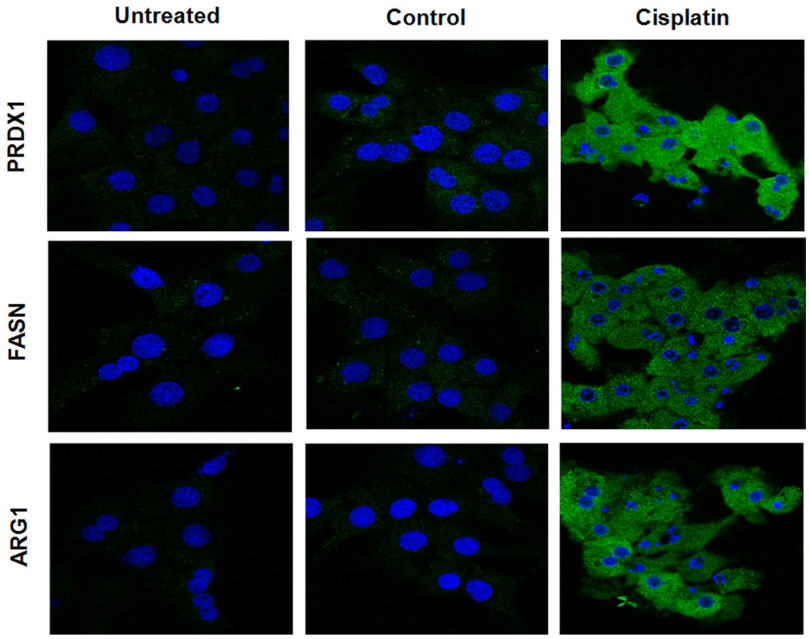

FIG. 5. **Immunofluorescence analysis of PRDX1, FASN, and ARG1 proteins.** Rat hepatocytes were treated with 0.1% Me_2SO (control) or 282.37 μM cisplatin (IC_{20}) for 24 h, respectively. The cells were incubated with the indicated antibodies. For detection, the cells were incubated with Alexa Fluor 488-labeled anti-rabbit secondary antibody. For nuclear staining, the cells were incubated with 4′,6′-diamino-2-phenylindole. The cells were washed and mounted with VECTASHIELD mounting medium. The images were collected using a confocal microscope. Cisplatin-treated hepatocytes caused an increase in PRDX1-, FASN-, and ARG1-specific staining.

plasma membrane proteins, which is easily not detected in proteomic analysis. In addition, the classification of 385 down-regulated genes based on biological functions showed binding proteins (82 genes), cytokines (14 genes), enzymes (58 genes), kinases (13 genes), peptidases (17 genes), phosphatases (9 genes), transcription regulators (81 genes), transmembrane receptors (21 genes), transporters (11 genes), and unknown (79 genes) (supplemental Table V*D*). Among 306 down-regulated genes excluding unknown genes (79 genes), 46% of genes encode low abundant proteins including cytokines, kinases, transcription regulators, transmembrane receptors, and transporters; their detection has been known to be challenging by the sensitivity of current proteomic tools. Furthermore, in this study, these down-regulated genes encoding membrane and low abundant proteins may cause translational down-regulation in protein level, which could enhance a difficulty in their detection by the proteomic analysis. Therefore, this analysis strongly suggests the necessity of identification of low abundance proteins with various proteomic technologies, such as subfractionation and two-dimensional LC methods to show more correlation between mRNA and protein levels.

In the present study, despite the different numbers of regulated genes and proteins, we observed that 73.1% among pathways affected in cisplatin-treated cells by proteomic analysis was detected by genomic analysis, which provides insight into the mechanisms of cisplatin-induced hepatotoxicity on well known pathways (drug metabolism, fatty acid metabolism, glycolysis, and TCA cycle) and little known pathways (urea cycle and inflammation metabolism) for hepatotoxicity of other toxic agents (Fig. 6). Many of these proteins and genes have associations with hepatotoxicity, and alteration of their interconnecting pathways could lead to deleterious effects on hepatocytes.

Expression of Proteins and Genes Associated with Drug Metabolism (CYP450 and Oxidative Stress Enzymes)—In this study, three proteins (CYP2D1, CYP2C13, and CYP2D5) and two genes (CYP2E1 and CYP4A1) were elevated in cisplatin-treated hepatocytes. Cytochrome P-450 (CYP) is known to be involved in metabolism of drugs, chemicals, and endogenous substrates. In addition, hepatic CYPs are involved in pathogenesis of several liver diseases (36, 37). Among them, elevated CYP2E1 has been reported to enhance cisplatin-induced hepatotoxicity, and increased ROS and oxidative stress are suggested as the toxic mechanisms *in vivo* (11, 38) and *in vitro* (11). Hence, the differential expression of other CYP isoforms identified in this study, CYP2D1, CYP2C13, CYP2D5, and CYP4A1, may explain toxic metabolism of cisplatin in hepatocytes.

The protein levels of these CYP450 enzymes are hardly detected in two-dimensional gel electrophoresis and LC-MS/MS method, probably because of low expression of CYP450 proteins. However, in this study, several isoforms of CYP450 enzymes were successfully identified probably because of a gel-assisted method (28), and IDEAL-Q software could aid in quantification of these proteins.

PRDX1 (peroxiredoxin 1) and PRDX5 proteins were up-regulated in the cisplatin-treated group as determined by LC-MS/MS analysis, and overexpression of PRDX1 was confirmed by Western blot and immunofluorescence analysis (Figs. 3 and 5). PRDX 1 and 5 participate in the signaling transduction cascades and modulation of cell proliferation/differentiation and cancer development or progression (39, 40). Based on proteomic analysis, acetaminophen, aminoda-

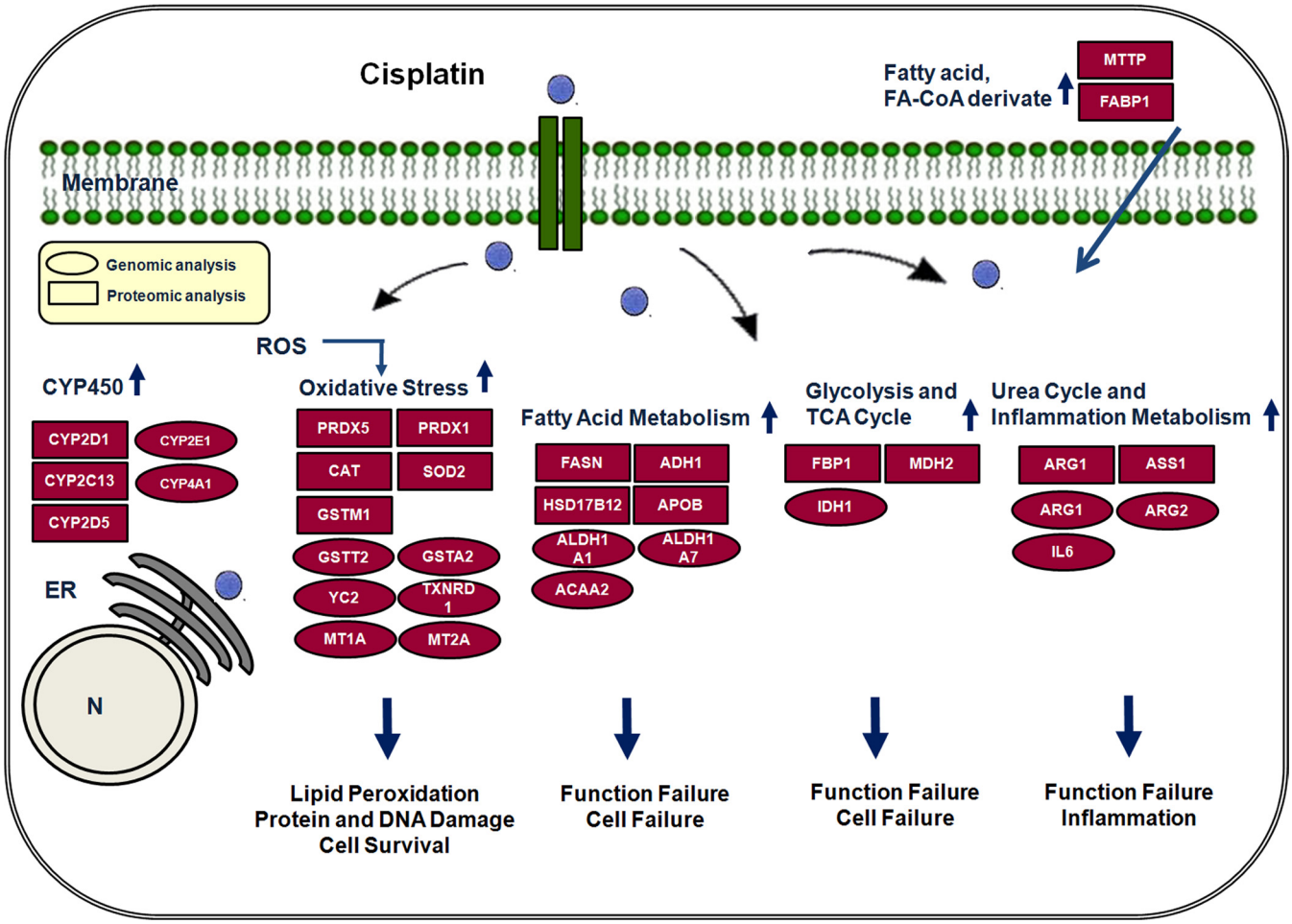

FIG. 6. **Pathway map related to cisplatin-induced hepatotoxicity based on proteomic and genomic analysis.** Mapping of ratios of proteins and genes on the drug metabolism, oxidative stress, fatty acid metabolism, glycolysis and TCA cycle, and urea cycle and inflammation metabolism. Networks of inter-relationships of these genes and proteins were constructed using the KEGG pathway program. The *rectangles* represent proteins obtained from the MS data. The *ovals* represent genes obtained from the microarray data.

rone, and tetracyclin induced hepatotoxicity and increased PRDX1 expression (41). These proteins were considered to be potential biomarkers of hepatotoxicity that would be more sensitive, reliable, and mechanism-based (41, 42). Therefore, PRDX1 and PRDX 5 might be important biomarkers in cisplatin-induced hepatocyte damage.

Up-regulation of proteins, such as CAT (catalase) and SOD2 (superoxide dismutase 2), indicated increased antioxidant responses in cisplatin-treated hepatocytes. A single oral dose of cyclosporine A in rats has been reported to induce marked hepatotoxicity, as well as antioxidant enzymes, including CAT and SOD2 (43). In addition, many studies have reported that drug toxicity is modulated by antioxidant enzymes (41, 42). Oxidative stress-related proteins are known to be controlled in redox regulation within hepatocytes.

Various glutathione *S*-transferase isoforms (GSTA2, GSTT2, and YC2) genes were significantly up-regulated in the cisplatin-treated group (Table III). GSTAs, a well reported family of phase II detoxification enzymes, catalyze conjugation of glutathione with reactive metabolites formed during phase I of metabolism (44–47). Rats treated with a single oral dose of either α-naphthylisothiocyanate, bromobenzene, or thioacetamide showed marked hepatotoxicity and GSTA elevation (48). GSTT3 and YC2 were predominantly expressed in the liver, playing a pivotal role in detoxification (49–51). D-Galactosamine-treated rats showed marked hepatotoxicity, with GSTT3 elevation (51). These accumulated data suggested that GSTs genes are responsible for cisplatin-induced hepatotoxicity.

mRNA expression of MT1A, MT2A, and TXNRD1 were increased in cisplatin-treated hepatocytes. Metallothionein has been proposed to play an important role in protection against hepatotoxicity produced by cadmium, and metallothionein-null mice were more sensitive than controls to cisplatin-induced hepatotoxicity, indicating the importance of constitutive metallothionein in protection against cisplatin-induced hepatotoxicity (52). TXNRD1 is an antioxidant enzyme in cytoplasm. Using genomic approaches, TXNRD1 was up-regu-

lated in the carbon tetrachloride- and acetaminophen-treated groups (53). Thus, because many oxidative stress-related proteins/genes were affected by cisplatin, our results confirmed that oxidative stress plays an important role in cisplatin-induced hepatotoxicity.

Expression of Proteins and Genes Associated with Fatty Acid Metabolism—Differential proteomic and genomic results showed up-regulation of six proteins (FASN, FABP1, ADH1, HSD17B12, MTTP, and APOB) and three genes (ALDH1A1, ALDH1A7, and ACAA2) related to fatty acid metabolism in cisplatin-treated cells. There are several reports on the deposition in the form of small lipid droplets in liver treated with hepatotoxic-inducing drugs, such as amiodarone (54) and cyclopropane carboxylic acid (55) and on fat accumulation by tetracycline treatment in mouse liver by reducing β-oxidation of fatty acids in mitochondria (56). Proteins such as FASN, FABP1, and HSD17B12 (estradiol 17-β-dehydrogenase 12) related to fatty acid synthesis were up-regulated and might contribute on the high level of fatty acid in cisplatin-treated hepatocytes. The overexpression of FASN protein, the sole protein in the human genome capable of reductive synthesis of long chain fatty acids from acetyl-coenzyme A (acetyl-CoA), malonyl CoA, and NADPH (57), was confirmed by Western blot and immunofluorescence analysis (Figs. 3 and 5). High expression of FASN in human carcinomas has been also reported (57, 58). MTTP (microsomal triglyceride transfer protein) and FABP1 were up-regulated by cisplatin as fatty acid transporter proteins. It has been reported that MTTP is a major target of carbon tetrachloride toxicity (59), and FABP1 is a target of acetaminophen toxicity (41). We also observed up-regulated proteins related to fatty acid β-oxidation such as peroxisomal ACOX2 (acyl-CoA oxidase 2), peroxisomal EHHADH (bifunctional enzyme), HADH (hydroxyacyl-CoA dehydrogenase), and ECHS1 (enoyl-CoA hydratase). The up-regulation of these proteins suggests that the peroxisome and mitochondria β-oxidation pathway might potentially compensate for the up-regulation of fatty acid synthesis. Therefore, these data suggested that up-regulation of these proteins could contribute to impair fatty acid metabolism in cisplatin-induced hepatotoxicity.

Two genes corresponding to isoenzymes of aldehyde dehydrogenase (ALDH1A1 and ALDH1A7) are up-regulated in cisplatin-treated cells. ALDH1A is a family of several isoenzymes that are important in cell defense against both exogenous and endogenous aldehydes (60). ALDH1A1 detoxifies cyclophosphamide, which belongs to the widely used oxazaphosphorine family of anticancer drugs (61). Microarray analysis of renal tissue after ischemia-reperfusion was reported to reveal a number of highly up-regulated antioxidant genes, including ALDH1A1 and ALDH1A7 (62). Thus, high expression of these genes may play detoxifying role in the cisplatin-induced hepatotoxicity.

Expression of Proteins and Genes Associated with Glycolysis and the TCA Cycle—FBP1, which is up-regulated in cisplatin-treated cells, catalyzes fructose 1,6-bisphosphate hydrolysis into fructose 6-phosphate and plays a critical role in glycolysis/gluconeogenesis. FBP1 has been reported as a single-stranded DNA-binding protein that activates the far upstream element of c-Myc (63), and FBP1 prevents endotoxemia and liver injury induced by D-galactosamine in rats through inhibition of macrophage activation (64). It was also shown that expression of FBP1 is increased to the threshold level of its anti-inflammatory action in response to a concanavalin A challenge (65). Therefore, FBP1 might play a role in influencing on the connection between DNA damage, aging, and oxidative stress through either direct signaling or an intricate adaptation in glycolysis.

Malate dehydrogenase, involved in the TCA cycle, is a leakage marker released into serum after tissue damage (66). Measurement of malate dehydrogenase activity is more useful in estimation of the severity of liver diseases than similar aspartate aminotransferase (66), and higher levels of malate dehydrogenase activity in cirrhotic patient sera, when compared with non-cirrhotic sera, were shown (67). According to one report, isocitrate dehydrogenase was related to toxicity and modulated by hexachlorocyclohexane-induced hepatocarcinogenesis in Swiss mice (68). Thus, these proteins are major enzymes that play roles in the TCA cycle and also could be leakage markers released in cisplatin-induced hepatotoxicity.

Expression of Proteins and Genes Associated with the Urea Cycle and Inflammation Metabolism—In mammals, there are two arginase isoenzymes, ARG1 and ARG2 (69). In this study, ARG1 enzyme was up-regulated in cisplatin-treated cells, as determined by MS analysis, and confirmed by Western blot and immunofluorescence analysis at the protein level (Figs. 3 and 5). ARG2 enzyme was also up-regulated at the mRNA level, as determined by microarray analysis and confirmed by RT-PCR (Fig. 4). ARG, mostly found in the liver, is a hydrolase that catalyzes the catabolism of arginine to urea and ornithine. ARG1 is a liver specific, making it a candidate biomarker that shows higher specificity, compared with liver enzymes (70). Hepatic ARG could serve as a useful marker for monitoring hepatic damage to the graft after liver transplantation (70).

ARG1 and ARG2 are emerging as key players in the mammalian immune system. ARG1 has been identified as the essential suppressive mediator of alternatively activated macrophages, demonstrating that ARG1 expressing macrophages function as suppressors rather than inducers of Th2-dependent inflammation and fibrosis (71). ARG2 is expressed in human PCa cells, and its inhibition increases the activation of tumor-infiltrating lymphocytes (71). Based on our results, we propose, for the first time, that ARG2 might also be related to hepatotoxicity similar to ARG1.

One of the urea cycle proteins, ASS1 (argininosuccinate synthase 1), was highly expressed in cisplatin-treated cells. Argininosuccinate synthase is an enzyme that catalyzes the synthesis of argininosuccinate from citrulline and aspartate.

Argininosuccinate synthase is also a potential biomarker of 3Z-3-[(1H-pyrrol-2-yl)-methylidene]-1-(1-piperidinylmethyl)-1,3–2H-indol-2-one-induced hepatotoxicity (72).

Molecular mediators of the immune response, such as TNF-α, IL-1β, and IL-6, are related to acute and chronic liver damage (73). The networks of these pro-inflammatory cytokines have been implicated in mediation of hepatic response to xenobiotics as diverse as peroxisome proliferator-activated receptor ligands, acetaminophen, and phenobarbital. These pro-inflammatory cytokines, such as TNF-α, IL-1β, and IL-6, are released into the bloodstream, both from the liver and distal sites during hepatotoxic injury. Thus, IL-6, which was up-regulated in this study, might be an important biomarker associated with inflammation pathways in cisplatin-induced hepatotoxicity.

Down-regulated Proteins and Genes—It has been reported that the inhibition of CTSB attenuates hepatic injury and fibrosis during cholestasis (74) and also protects against cell death in nonsmall cell lung cancer (75). This protease is released from lysosomes into the cytosol by cytotoxic-signal cascades and is known as a candidate target for inhibiting hepatocyte apoptosis in liver disease. Therefore, the down-regulation of CTSB in cisplatin-treated primary hepatocyte could be a defense mechanism to survive in a hepatotoxic situation.

TPM isoforms are ubiquitous proteins associated with actin filaments in muscle and nonmuscle cells (76). In hepatocytes, TPM plays a role in stabilization of actin filaments (77). It has been reported that there is decreased expression of TPM in proteomic analysis of hepatocellular carcinoma (77) and in human ovarian cancer tissues (78). The treatment of cisplatin, in this study, decreased the expression of TPM1 and TPM3, and it could destabilize actin filaments. We could assume that TPM may be involved in destruction of hepatocytes after cisplatin-induced injury.

In this study, mRNA expression of CYP2C12 and CYP26B1 was reduced in cisplatin-treated hepatocytes. CYP2C12 has been known as one of female-specific sex-predominant isoforms (79), and the function of CYP2C12 in male rats has not been reported. However, there is one report showing the induction of CYP2C12 in senescent male rats (80). CYP26B1 has been studied mostly in development and brain researches. CYP26B1 is regulated by retinoic acid and essential for germ cell development and postnatal survival (81). Therefore, further study to understand the relationship between hepatotoxicity and the two CYP isoforms is warranted.

Conclusion—We described the proteomics and genomics profiles of rat primary hepatocytes treated with cisplatin using nano LC-MS/MS and microarray, respectively. Many liver proteins and pathways modulated in the response to cisplatin were identified in the present study. Among the defined pathways, we focused on some pathways including drug metabolism, fatty acid metabolism, glycolysis and TCA cycle, urea cycle, and inflammation metabolism pathways. Pathway and network analyses provided an integrated picture of the hepatotoxic effects of cisplatin in rat hepatocytes. By comparing proteomic profiles with genomic profiles, the present study provides information useful for an understanding of the roles of these alterations in regard to the cytotoxicity and toxic mechanisms of cisplatin. Finally, this study represents the first application of both proteomic and genomic analysis on cisplatin-treated rat primary hepatocytes and provides novel insight into the potential toxic pathways induced by cisplatin.

* This is work was supported by Korea Food and Drug Administration Grant 09172KFDA641 and a grant from the Korean Ministry of Education, Science and Technology (The Regional Core Research Program/Anti-aging and Well-being Research Center).The costs of publication of this article were defrayed in part by the payment of page charges. This article must therefore be hereby marked "*advertisement*" in accordance with 18 U.S.C. Section 1734 solely to indicate this fact.

[S] This article contains supplemental Tables I–V and Figs. 1–3.

‡‡ These two senior authors contributed equally.

§§ To whom correspondence should be addressed: Dept. of Molecular Medicine, School of Medicine, Kyungpook National University, 101 Dongin-dong 2Ga, Jung-Gu, Daegu 700-422, Republic of Korea. Fax: +82-53-426-4944; E-mail: mcbaek@knu.ac.kr.

REFERENCES

1. van Basten, J. P., Schrafford Koops, H., Sleijfer, D. T., Pras, E., van Driel, M. F., and Hoekstra, H. J. (1997) Current concept about testicular cancer. *Eur. J. Surg. Oncol.* **23,** 354–360
2. Saad, S. Y., Najjar, T. A., Noreddin, A. M., and Al-Rikabi, A. C. (2001) Effects of gemcitabine on cisplatin-induced nephrotoxicity in rats: Schedule-dependent study. *Pharmacol. Res.* **43,** 193–198
3. Madias, N. E., and Harrington, J. T. (1978) Platinum nephrotoxicity. *Am. J. Med.* **65,** 307–314
4. Cersosimo, R. J. (1993) Hepatotoxicity associated with cisplatin chemotherapy. *Ann. Pharmacother.* **27,** 438–441
5. Zicca, A., Cafaggi, S., Mariggiò, M. A., Vannozzi, M. O., Ottone, M., Bocchini, V., Caviglioli, G., and Viale, M. (2002) Reduction of cisplatin hepatotoxicity by procainamide hydrochloride in rats. *Eur. J. Pharmacol.* **442,** 265–272
6. Cavalli, F., Tschopp, L., Sonntag, R. W., and Zimmermann, A. (1978) Cisplatin-induced hepatic toxicity. *Cancer Treat. Rep.* **62,** 2125–2126
7. Liao, Y., Lu, X., Lu, C., Li, G., Jin, Y., and Tang, H. (2008) Selection of agents for prevention of cisplatin-induced hepatotoxicity. *Pharmacol. Res.* **57,** 125–131
8. Naziroglu, M., Karaoğlu, A., and Aksoy, A. O. (2004) Selenium and high dose vitamin E administration protects cisplatin-induced oxidative damage to renal, liver and lens tissues in rats. *Toxicology* **195,** 221–230
9. Iraz, M., Kalcioglu, M. T., Kizilay, A., and Karatas, E. (2005) Aminoguanidine prevents ototoxicity induced by cisplatin in rats. *Ann. Clin. Lab. Sci.* **35,** 329–335
10. Işeri, S., Ercan, F., Gedik, N., Yüksel, M., and Alican, I. (2007) Simvastatin attenuates cisplatin-induced kidney and liver damage in rats. *Toxicology* **230,** 256–264
11. Lu, Y., and Cederbaum, A. I. (2006) Cisplatin-induced hepatotoxicity is enhanced by elevated expression of cytochrome P450 2E1. *Toxicol. Sci.* **89,** 515–523
12. Lee, W. M. (2003) Drug-induced hepatotoxicity. *N. Engl. J. Med.* **349,** 474–485
13. Wetmore, B. A., and Merrick, B. A. (2004) Toxicoproteomics: Proteomics applied to toxicology and pathology. *Toxicol. Pathol.* **32,** 619–642
14. Bissell, D. M., Gores, G. J., Laskin, D. L., and Hoofnagle, J. H. (2001) Drug-induced liver injury: Mechanisms and test systems. *Hepatology* **33,** 1009–1013
15. Holt, M. P., and Ju, C. (2006) Mechanisms of drug-induced liver injury. *AAPS J.* **8,** E48–E54
16. Russmann, S., Kullak-Ublick, G. A., and Grattagliano, I. (2009) Current

concepts of mechanisms in drug-induced hepatotoxicity. *Curr. Med. Chem.* **16,** 3041–3053
17. Takikawa, H. (2009) Recent status of drug-induced liver injury. *Hepatol. Res.* **39,** 1–6
18. Park, B. K., Kitteringham, N. R., Maggs, J. L., Pirmohamed, M., and Williams, D. P. (2005) The role of metabolic activation in drug-induced hepatotoxicity. *Annu. Rev. Pharmacol. Toxicol.* **45,** 177–202
19. Collins, B. C., Clarke, A., Kitteringham, N. R., Gallagher, W. M., and Pennington, S. R. (2007) Use of proteomics for the discovery of early markers of drug toxicity. *Expert Opin. Drug. Metab. Toxicol.* **3,** 689–704
20. Deganuto, M., Cesaratto, L., Bellarosa, C., Calligaris, R., Vilotti, S., Renzone, G., Foti, R., Scaloni, A., Gustincich, S., Quadrifoglio, F., Tiribelli, C., and Tell, G. (2010) A proteomic approach to the bilirubin-induced toxicity in neuronal cells reveals a protective function of DJ-1 protein. *Proteomics* **10,** 1645–1657
21. Hammer, E., Bien, S., Salazar, M. G., Steil, L., Scharf, C., Hildebrandt, P., Schroeder, H. W., Kroemer, H. K., Völker, U., and Ritter, C. A. (2010) Proteomic analysis of doxorubicin-induced changes in the proteome of HepG2cells combining 2-D DIGE and LC-MS/MS approaches. *Proteomics* **10,** 99–114
22. Ruepp, S. U., Tonge, R. P., Shaw, J., Wallis, N., and Pognan, F. (2002) Genomics and proteomics analysis of acetaminophen toxicity in mouse liver. *Toxicol. Sci.* **65,** 135–150
23. Ortiz, P. A., Bruno, M. E., Moore, T., Nesnow, S., Winnik, W., and Ge, Y. (2010) Proteomic analysis of propiconazole responses in mouse liver: Comparison of genomic and proteomic profiles. *J. Proteome Res.* **9,** 1268–1278
24. Tsou, C. C., Tsai, C. F., Tsui, Y. H., Sudhir, P. R., Wang, Y. T., Chen, Y. J., Chen, J. Y., Sung, T. Y., and Hsu, W. L. (2010) IDEAL-Q, an automated tool for label-free quantitation analysis using an efficient peptide alignment approach and spectral data validation. *Mol. Cell. Proteomics* **9,** 131–144
25. Wang, Y. T., Tsai, C. F., Hong, T. C., Tsou, C. C., Lin, P. Y., Pan, S. H., Hong, T. M., Yang, P. C., Sung, T. Y., Hsu, W. L., and Chen, Y. J. (2010) An informatics-assisted label-free quantitation strategy that depicts phosphoproteomic profiles in lung cancer cell invasion. *J. Proteome Res.* **9,** 5582–5597
26. Han, C. L., Chen, J. S., Chan, E. C., Wu, C. P., Yu, K. H., Chen, K. T., Tsou, C. C., Tsai, C. F., Chien, C. W., Kuo, Y. B., Lin, P. Y., Yu, J. S., Hsueh, C., Chen, M. C., Chan, C. C., Chang, Y. S., and Chen, Y. J. (2011) An Informatic-assisted label-free approach for personalized tissue membrane proteomics: Case study on colorectal cancer. *Mol. Cell. Proteomics* **10,** 10.1074/mcp.M110.003087
27. Figliomeni, M. L., and Abdel-Rahman, M. S. (1998) Ethanol does not increase the hepatotoxicity of cocaine in primary rat hepatocyte culture. *Toxicology* **129,** 125–135
28. Han, C. L., Chien, C. W., Chen, W. C., Chen, Y. R., Wu, C. P., Li, H., and Chen, Y. J. (2008) A multiplexed quantitative strategy for membrane proteomics: Opportunities for mining therapeutic targets for autosomal dominant polycystic kidney disease. *Mol. Cell. Proteomics* **7,** 1983–1997
29. Rowe, C., Goldring, C. E., Kitteringham, N. R., Jenkins, R. E., Lane, B. S., Sanderson, C., Elliott, V., Platt, V., Metcalfe, P., and Park, B. K. (2010) Network analysis of primary hepatocyte dedifferentiation using a shotgun proteomics approach. *J. Proteome Res.* **9,** 2658–2668
30. Lee, M. H., Hong, I., Kim, M., Lee, B. H., Kim, J. H., Kang, K. S., Kim, H. L., Yoon, B. I., Chung, H., Kong, G., and Lee, M. O. (2007) Gene expression profiles of murine fatty liver induced by the administration of valproic acid. *Toxicol. Appl. Pharmacol.* **220,** 45–59
31. Huber, W., Heydebreck, A., Sultmann, H., Poustka, A., and Vingron, M. (2002) Variance stabilization applied to microarray data calibration and to the quantification of differential expression. *Bioinformatics* **18,** 96–104
32. Bolstad, B. M., Irizarry, R. A., Astrand, M., and Speed, T. P. (2003) A comparison of normalization methods for high density oligonucleotide array data based on variance and bias. *Bioinformatics* **22,** 185–193
33. Klipper-Aurbach, Y., Wasserman, M., Braunspiegel-Weintrob, N., Borstein, D., Peleg, S., Assa, S., Karp, M., Benjamini, Y., Hochberg, Y., and Laron, Z. (1995) Mathematical formulae for the prediction of the residual beta cell function during the first two years of disease in children and adolescents with insulin-dependent diabetes mellitus. *Med. Hypotheses* **45,** 486–490
34. Craig, A., Sidaway, J., Holmes, E., Orton, T., Jackson, D., Rowlinson, R., Nickson, J., Tonge, R., Wilson, I., and Nicholson, J. (2006) Systems toxicology: Integrated genomic, proteomic and metabonomic analysis of methapyrilene induced hepatotoxicity in the rat. *J. Proteome Res.* **5,** 1586–1601
35. Nie, L., Wu, G., Culley, D. E., Scholten, J. C., and Zhang, W. (2007) Integrative analysis of transcriptomic and proteomic data: challenges, solutions and applications. *Crit. Rev. Biotechnol.* **27,** 63–75
36. Juran, B. D., Egan, L. J., and Lazaridis, K. N. (2006) The AmpliChip CYP450 test: Principles, challenges, and future clinical utility in digestive disease. *Clin. Gastroenterol. Hepatol.* **4,** 822–830
37. Jia, N., Liu, X., Wen, J., Qian, L., Qian, X., Wu, Y., and Fan, G. (2007) A proteomic method for analysis of CYP450s protein expression changes in carbon tetrachloride induced male rat liver microsomes. *Toxicology* **237,** 1–11
38. Neuwelt, A. J., Wu, Y. J., Knap, N., Losin, M., Neuwelt, E. A., Pagel, M. A., Warmann, S., Fuchs, J., Czauderna, P., and Wozniak, M. (2009) Using acetaminophen's toxicity mechanism to enhance cisplatin efficacy in hepatocarcinoma and hepatoblastoma cell lines. *Neoplasia* **11,** 1003–1111
39. Immenschuh, S., and Baumgart-Vogt, E. (2005) Peroxiredoxins, oxidative stress, and cell proliferation. *Antioxid. Redox Signal.* **7,** 768–777
40. Cesaratto, L., Vascotto, C., D'Ambrosio, C., Scaloni, A., Baccarani, U., Paron, I., Damante, G., Calligaris, S., Quadrifoglio, F., Tiribelli, C., and Tell, G. (2005) Overoxidation of peroxiredoxins as an immediate and sensitive marker of oxidative stress in HepG2 cells and its application to the redox effects induced by ischemia/reperfusion in human liver. *Free Radic. Res.* **39,** 255–268
41. Yamamoto, T., Kikkawa, R., Yamada, H., and Horii, I. (2005) Identification of oxidative stress-related proteins for predictive screening of hepatotoxicity using a proteomic approach. *J. Toxicol. Sci.* **30,** 213–227
42. Yamamoto, T., Tomizawa, K., Fujikawa, M., Sato, Y., Yamada, H., and Horii, I. (2007) Evaluation of human hepatocyte chimeric mice as a model for toxicological investigation using panomic approaches: Effect of acetaminophen on the expression profiles of proteins and endogenous metabolites in liver, plasma and urine. *J. Toxicol. Sci.* **32,** 205–215
43. Erarslan, E., Ekiz, F., Uz, B., Koca, C., Turkcu, U. O., Bayrak, R., and Delibasi, T. (2011) Effects of erdosteine on cyclosporine A-induced hepatotoxicity in rats. *Drug Chem. Toxicol.* **34,** 32–37
44. Kaplowitz, N. (1980) Physiological significance of the glutathione *S*-transferases. *Am. J. Physiol.* **239,** G439–G444
45. Hayes, J. D., and Pulford, D. J. (1995) The glutathione *S*-transferase supergene family: Regulation of GST and the contribution of the isoenzymes to cancer chemoprotection and drug resistance. *Crit. Rev. Biochem. Mol. Biol.* **30,** 445–600
46. Chiou, H. Y., Hsueh, Y. M., Hsieh, L. L., Hsu, L. I., Hsu, Y. H., Hsieh, F. I., Wei, M. L., Chen, H. C., Yang, H. T., Leu, L. C., Chu, T. H., Chen-Wu, C., Yang, M. H., and Chen, C. J. (1997) Arsenicmethylation capacity, body retention, and null genotypes of glutathione *S*-transferase M1 and T1 among current arsenic-exposed residents in Taiwan. *Mutat. Res.* **386,** 197–207
47. Strange, R. C., Jones, P. W., and Fryer, A. A. (2000) Glutathione *S*-transferase: Genetics and role in toxicology. *Toxicol. Lett.* **112–113,** 357–363
48. Giffen, P. S., Turton, J., Andrews, C. M., Barrett, P., Clarke, C. J., Fung, K. W., Munday, M. R., Roman, I. F., Smyth, R., Walshe, K., and York, M. J. (2003) Markers of experimental acute inflammation in the Wistar Han rat with particular reference to haptoglobin and creactive protein. *Arch. Toxicol.* **77,** 392–402
49. Coggan, M., Flanagan, J. U., Parker, M. W., Vichai, V., Pearson, W. R., and Board, P. G. (2002) Identification and characterization of GSTT3, a third murine Theta class glutathione transferase. *Biochem. J.* **366,** 323–332
50. Knight, T. R., Choudhuri, S., and Klaassen, C. D. (2008) Induction of hepatic glutathione *S*-transferases in male mice by prototypes of various classes of microsomal enzyme inducers. *Toxicol. Sci.* **106,** 329–338
51. Yun, J. W., Kim, C. W., Bae, I. H., Park, Y. H., Chung, J. H., Lim, K. M., and Kang, K. S. (2010) Expression levels of pituitary tumor transforming 1 and glutathione *S*-transferase theta 3 are associated with the individual susceptibility to D-galactosamine-induced hepatotoxicity. *Toxicol. Appl. Pharmacol.* **242,** 91–99
52. Liu, J., Liu, Y., Habeebu, S. S., and Klaassen, C. D. (1998) Metallothionein (MT)-null mice are sensitive to cisplatin-induced hepatotoxicity. *Toxicol. Appl. Pharmacol.* **149,** 24–31

53. Fukushima, T., Kikkawa, R., Hamada, Y., and Horii, I. (2006) Genomic cluster and network analysis for predictive screening for hepatotoxicity. *J. Toxicol. Sci.* **31,** 419–432
54. Fromenty, B., Fisch, C., Labbe, G., Degott, C., Deschamps, D., Berson, A., Letteron, P., and Pessayre, D. (1990) Amiodarone inhibits the mitochondrial beta-oxidation of fatty acids and produces microvesicular steatosis of the liver in mice. *J. Pharmacol. Exp. Ther.* **255,** 1371–1376
55. Jolly, R. A., Ciurlionis, R., Morfitt, D., Helgren, M., Patterson, R., Ulrich, R. G., and Waring, J. F. (2004) Microvesicular steatosis induced by a short chain fatty acid: Effects on mitochondrial function and correlation with gene expression. *Toxicol. Pathol.* **32,** 19–25
56. Yin, H. Q., Kim, M., Kim, J. H., Kong, G., Lee, M. O., Kang, K. S., Yoon, B. I., Kim, H. L., and Lee, B. H. (2006) Hepatic gene expression profiling and lipid homeostasis in mice exposed to steatogenic drug, tetracycline. *Toxicol. Sci.* **94,** 206–216
57. Wakil, S. J. (1989) Fatty-acid synthase, a proficient multifunctional enzyme. *Biochemistry* **28,** 4523–4530
58. Kuhajda, F. P. (2006) Fatty acid synthase and cancer: New application of an old pathway. *Cancer Res.* **66,** 5977–5980
59. Pan, X., Hussain, F. N., Iqbal, J., Feuerman, M. H., and Hussain, M. M. (2007) Inhibiting proteasomal degradation of microsomal triglyceride transfer protein prevents CCl4-induced steatosis. *J. Biol. Chem.* **282,** 17078–17089
60. Marchitti, S. A., Deitrich, R. A., and Vasiliou, V. (2007) Neurotoxicity and metabolism of the catecholamine-derived 3,4-dihydroxyphenylacetaldehyde and 3,4-dihydroxyphenylglycolaldehyde: the role of aldehyde dehydrogenase. *Pharmacol. Rev.* **59,** 125–150
61. Manthey, C. L., Landkamer, G. J., and Sladek, N. E. (1990) Identification of the mouse aldehyde dehydrogenases important in aldophosphamide detoxification. *Cancer Res.* **50,** 4991–5002
62. Leonard, M. O., Kieran, N. E., Howell, K., Burne, M. J., Varadarajan, R., Dhakshinamoorthy, S., Porter, A. G., O'Farrelly, C., Rabb, H., and Taylor, C. T. (2006) Reoxygenation-specific activation of the antioxidant transcription factor Nrf2 mediates cytoprotective gene expression in ischemia-reperfusion injury. *FASEB J.* **20,** 2624–2626
63. Duncan, R., Bazar, L., Michelotti, G., Tomonaga, T., Krutzsch, H., Avigan, M., and Levens, D. (1994) A sequence-specific, single-strand binding protein activates the far upstream element of c-myc and defines a new DNA-binding motif. *Genes Dev.* **8,** 465–480
64. Cuesta, E., Boada, J., Calafell, R., Perales, J. C., Roig, T., and Bermudez, J. (2006) Fructose 1,6-bisphosphate prevented endotoxemia, macrophage activation, and liver injury induced by D-galactosamine in rats. *Crit. Care Med.* **34,** 807–814
65. Tan, X. F., Chen, F., Wu, S. S., Shi, Y., Liu, D. C., and Chen, Z. (2010) Science letters: Proteomic analysis of differentially expressed proteins in mice with concanavalin A-induced hepatitis. *J. Zhejiang. Univ. Sci. B.* **11,** 221–226
66. Ozer, J., Ratner, M., Shaw, M., Bailey, W., and Schomaker, S. (2008) The current state of serum biomarkers of hepatotoxicity. *Toxicology* **245,** 194–205
67. Misra, M. K., Khanna, A. K., Sharma, R., and Srinivasan, S. (1991) Serum malate dehydrogenase (MDH) in portal hypertension: Its value as a diagnostic and prognostic indicator. *Indian J. Med. Sci.* **45,** 31–34
68. Bhatt, D. K., and Bano, M. (2009) Modulation of tricarboxylic acid cycle dehydrogenases during hepatocarcinogenesis induced by hexachlorocyclohexane in mice. *Exp. Toxicol. Pathol.* **61,** 325–332
69. Jenkinson, C. P., Grody, W. W., and Cederbaum, S. D. (1996) Comparative properties of arginases. *Comp. Biochem. Physiol. B. Biochem. Mol. Biol.* **114,** 107–132
70. Ashamiss, F., Wierzbicki, Z., Chrzanowska, A., Scibior, D., Pacholczyk, M., Kosieradzki, M., Lagiewska, B., Porembska, Z., and Rowiński, W. (2004) Clinical significance of arginase after liver transplantation. *Ann. Transplant.* **9,** 58–60
71. Munder, M. (2009) Arginase: an emerging key player in the mammalian immune system. *Br. J. Pharmacol.* **158,** 638–651
72. Wang, Y., Yang, B., Wu, C., Zheng, Z., Yuan, Y., Hu, Z., Ma, H., Li, S., Liao, M., and Wang, Q. (2010) Plasma and liver proteomic analysis of 3Z-3-[(1H-pyrrol-2-yl)-methylidene]-1-(1-piperidinylmethyl)-1,3–2H-indol-2-one-induced hepatotoxicity in Wistar rats. *Proteomics* **10,** 2927–2941
73. Lacour, S., Gautier, J. C., Pallardy, M., and Roberts, R. (2005) Cytokines as potential biomarkers of liver toxicity. *Cancer Biomark.* **1,** 29–39
74. Canbay, A., Guicciardi, M. E., Higuchi, H., Feldstein, A., Bronk, S. F., Rydzewski, R, Taniai, M., and Gores, G. J. (2003) Cathepsin B inactivation attenuates hepatic injury and fibrosis during cholestasis. *J. Clin. Invest.* **112,** 152–159
75. Bröker, L. E., Huisman, C., Span, S. W., Rodriguez, J. A., Kruyt, F. A., and Giaccone, G. (2004) Cathepsin B mediates caspase-independent cell death induced by microtubule stabilizing agents in non-small cell lung cancer cells. *Cancer Res.* **64,** 27–30
76. Mölleken, C., Sitek, B., Henkel, C., Poschmann, G., Sipos, B., Wiese, S., Warscheid, B., Broelsch, C., Reiser, M., Friedman, S. L., Tornøe, I., Schlosser, A., Klöppel, G., Schmiegel, W., Meyer, H. E., Holmskov, U., and Stühler, K. (2009) Detection of novel biomarkers of liver cirrhosis by proteomic analysis. *Hepatology* **49,** 1257–1266
77. Yokoyama, Y., Kuramitsu, Y., Takashima, M., Iizuka, N., Toda, T., and Terai, S. (2004) Proteomic profiling of proteins decreased in hepatocellular carcinoma from patients infected with hepatitis C virus. *Proteomics* **24,** 2111–2116
78. Alaiya, A. A., Franzén, B., Fujioka, K., Moberger, B., Schedvins, K., Silfversvärd, C., Linder, S., and Auer, G. (1997) Phenotypic analysis of ovarian carcinoma: Polypeptide expression in benign, borderline and malignant tumors. *Int. J. Cancer.* **73,** 678–783
79. Lin, J. H., and Lu, A. Y. (1997) Role of pharmacokinetics and metabolism in drug discovery and development. *Pharmacol. Rev.* **49,** 403–449
80. Wauthier, V., Dubois, P., Verbeeck, R. K., and Calderon, P. B. (2007) Induction of CYP2C12 expression in senescent male rats is well correlated to an increase of HNF3beta expression, while the decline of CYP2C11 expression is unlikely due to a decrease of STAT5 activation. *Biochem. Pharmacol.* **73,** 923–933
81. Ross, A. C., and Zolfaghari, R. (2011) Cytochrome P-450s in the regulation of cellular retinoic Acid metabolism. *Annu. Rev. Nutr.* **31,** 65–87